Mapping Snow Pack Depth in the Town of Uxbridge, Ontario Using an Airborne Laser Scanner

by

Jason Oldham

A thesis
presented to the University of Waterloo
in fulfillment of the
thesis requirement for the degree of
Master of Science
in
Geography

Waterloo, Ontario, Canada, 2011

I hereby declare that I am the sole author of this thesis. This is a true copy of the thesis, including any required final revisions, as accepted by my examiners.

I understand that my thesis may be made electronically available to the public.

Abstract

This study aims to present and evaluate a new method for measuring the distribution of snow within built-up environments by differencing elevations collected by an Airborne Laser Scanner (ALS) before, and during peak snow accumulation.

Few efforts have been made to study the distribution of snow within built-up environments due to the false assumption that high-intensity rainfall is the main contributor to peak yearly runoff rates. Traditional techniques for measuring snow are often difficult to replicate in built-up environments due to incompatibility of methods and barriers such as buildings, roads and private property. Light Detection and Ranging (LiDAR) technology, specifically ALSs, have previously been used to characterize the distribution of snow under forest canopy, and in remote mountain environments. This study investigates and assesses the utility of high resolution, non-intrusive ALS data for estimating the depth and distribution of snow within the town of Uxbridge, Ontario.

ALS flights for this study were completed before the onset of snow accumulation, as well as near peak snow accumulation for the winters of 2010 and 2011. Pre and post snow accumulation ALS measured elevations were differenced to estimate the depth of the snowpack across the entire study area at a resolution of 0.5 m. Ground measurements of snow depth were also completed within 24 hours of each of the winter flights. The LiDAR-estimated and ground-measured snow depths were compared using Spearman's rank correlation coefficient as well as Mean Absolute Error (MAE) and Root Mean Squared Error (RMSE).

Results from this thesis show that: 1) Snow depths estimated by differencing elevations from two ALS flights show a MAE of 3 cm and an RMSE of 10 cm when compared to ground-measured snow depths. (2) There is a strong, statistically significant relationship ($\rho = 0.82$, p < 0.001) between LiDAR-estimated and ground-measured snow depths. (3) An average bias of -3 cm was found for the entire dataset showing an underestimation in the LiDAR-estimated snow depths most likely caused by the effects of low lying vegetation on the fall ALS measurements.

The results presented in this study demonstrate that ALSs are capable of providing high spatial resolution snow depth estimates within built-up environments. Furthermore, snow depth measurements made using an ALS can be used to increase the current body of knowledge on the distribution and re-distribution of snow within built-up environments. Snow distributions measured by an ALS could also be used for future development and verification of urban hydrological models.

Acknowledgements

First and foremost, I would not have completed this thesis without the support of my many friends and family through the past two years. For the data collection and processing, I would like to thank those who helped at Optech most notably, Glenn Farrigton and Troy Lane for letting me collect the data for my thesis, Matthew Slater, and Rudy Zutis for flying the ALTMs, and Chris Richards for his speedy QAQC of the LiDAR data. My Father, and Murray both deserve thanks for making me a snow depth probe at the last minute (even though it was imperial!). I would like to thank all of my friends at Waterloo for being critical of my work and helping me push myself to finish. Last but definitely not least I should thank Richard Kelly, Claude Duguay, and Alex Brenning for their help throughout, but especially in the final stages of completing my thesis.

THANKS!!!

Dedication

This thesis is dedicated to family and friends. Thanks for the support!

Table of Contents

List of Tables

List of Figures

List of Acronyms

1 PPS   1 Pulse Per Second

ALS   Airborne Laser Scanner

ALTM   Airborne Laser Terrain Mapper

BRDF   Bidirectional Reflection Distribution Function

DEM   Digital Elevation Model

DSM   Digital Surface Model

GPS   Global Positioning System

IMU   Inertial Measurement Unit

LAS file Laser file

LiDAR   Light Detection and Ranging

MAE   Mean Absolute Error

POS   Position Orientation System

RMSE   Root Mean Squared Error

SWE   Snow Water Equivalent

TIN   Triangular Irregular Network

TLS   Terrestrial Laser Scanner

WGS84 World Geodetic System 1984

Chapter 1

Introduction

Airborne laser scanning also known as Light Detection and Ranging (LiDAR) is a remote sensing tool capable of measuring hundreds of thousands of high accuracy elevation points per second over varying terrain and land cover types. The speed at which Airborne Laser Scanners (ALSs) can collect and output data make them a valuable tool for flood mapping, 3D urban modeling and many other applications (Wehr and Lohr, 1999). When ALS data is collected before and after snow accumulation, the two datasets can be differenced to create a high resolution snow depth map with vertical resolution in the decimeter range (Deems and Painter, 2006; Hopkinson et al., 2004; Moreno Baños et al., 2011). Studies that have been completed to date on the use of ALSs for measuring snow depth have been in forested areas (Hopkinson et al., 2004), and mountainous terrain (Deems et al., 2006; Deems and Painter, 2006; Egli et al., 2011; Moreno Baños et al., 2011). Although several studies have used ALSs to estimate snow depth, few validations of LiDAR-estimated depths using *in situ* measurements have been completed (Moreno Baños et al., 2011). Presently, there has been no work completed on the use or validation of ALSs for estimating snow depths in built-up environments.

Snow in built-up environments is often looked at as a hazard or a nuisance. Large snow events can cripple entire cities for days at a time, costing millions of dollars in removal costs and shutdowns(Boyd et al., 1981). The city of Toronto alone has a budget of $82 million for snow removal in 2011 (City of Toronto, 2011). Snowmelt near the end of the winter season is a contributor to flooding in built-up environments and can be a cause of pollution in nearby watercourses (Viklander et al., 2003). To date there have been few studies completed on quantifying the amount of snow that falls within built-up environments or how the snow pack is distributed and re-distributed throughout the winter season (Ho and Valeo, 2005). A better understanding of how snow is distributed in built-up environments would help to better plan for the management of snow after it has fallen as well as during spring melt.

Measuring the distribution and characteristics of snow in rural and remote areas can be done using several manual and automated approaches. Current methods used for measuring snow distribution in rural areas include using snow stakes, snow depth transects (usually $\geq$ 100 m) and groups of instruments such as snow pillows or ultrasonic distance sensors(Elder et al., 2009a; Matheussen and Thorolfsson, 2001). These measurements, however, are often time consuming, expensive, can be dangerous, and disturb the snow pack possibly influencing future measurements (Deems and Painter, 2006). When applied to built-up areas many of these methods become more difficult or even impossible due to obstacles such as traffic, buildings, roads, and private property (Matheussen and Thorolfsson, 2001).

Several automated remote sensing methods, such as microwave remote sensing and satellite imagery are also available for measuring snow cover. Unfortunately, these instruments either lack the spatial resolution needed to measure snow in an urban environment, or are only capable of providing the areal extent of snow cover and not the amount (Rango, 1996). Limitations with the traditional methods above, make the use of a non-intrusive,

2

high resolution method such as LiDAR ideal for measuring the distribution of snow in built-up environments.

1.1   Research Objectives

The objective of this thesis is to present and evaluate a new method for measuring the distribution of snow depths within built-up environments by differencing elevations collected by an Airborne Laser Scanner before, and during peak snow accumulation.

To evaluate the use of ALSs for measuring the distribution of snow, three ALS flights were completed between the October 2009 and February 2011 over the town of Uxbridge, Ontario. The first flight was completed in October 2009, before snow accumulation began, while the other two were completed near peak accumulation during the winters of 2010 and 2011. *In situ* snow depth measurements were made within 24 hours of each of the ALS flights for comparison with the snow depth values estimated using the LiDAR data. To assess the accuracy of the ALS at estimating snow depths the *in situ* measurements were compared with the LiDAR-estimated snow depths using Mean Absolute Error (MAE), Root Mean Squared Error (RMSE) and a correlation coefficient. The evaluation of this new method of measuring snow in built-up environments are presented in chapters 4 and 5.

1.2   Outline of Thesis

A comprehensive literature review is presented in chapter 2 which provides context and background for this research. Chapter 3 provides an overview of the study area as well as a

detailed description of the methods used during this study. In Chapter 4, estimated snow depth maps are presented along with the results of an accuracy assessment of the LiDAR-estimated snow depth maps. Chapter 5 is a discussion of the results presented in Chapter 4 along with discussion of possible causes of errors, and limitations of the study; suggestions for future work are also presented in this chapter. Chapter 6 outlines conclusions presented throughout the results and discussion sections of this thesis.

Chapter 2

Literature Review and Research Context

This chapter provides background and research context for the methods used and discussed in this study. An overview of ALSs, how they work and the uncertainties present in the measurements they make is presented. A description of the factors that influence the distribution of snow as well as how these are effected by built-up environments is then presented. Current methods for measuring snow are then discussed followed by an overview of LiDAR-snow surface interactions. Previous studies related to the methods presented in this thesis are then discussed with a description of how they relate to this study.

2.1   Overview of Airborne Laser Scanning

ALSs or airborne LiDAR instruments are products created from the integration of several subsystems with an end goal of measuring geographically referenced points representing the elevation of objects on or near the ground. The main components of a standard ALS are: a

laser range-finder, scanning system, Position Orientation System (POS), and a controlling computer (Wehr and Lohr, 1999). The role of each of these subsystems, how they function, and potential sources of error will be discussed in this section

Laser range-finding, also know as Light Detection and Ranging (LiDAR) is a method of measuring the range to a distant object using a laser. To determine the distance to an object, a LiDAR system emits a laser pulse and records the amount of time until backscatter from that pulse returns from a remote surface (Baltsavias, 1999; Wehr and Lohr, 1999). Modern LiDAR systems are capable of emitting pulses at rates >200 kHz with up to four return pulses being recorded for each pulse emitted (Optech Inc., 2011c). To complete this measurement a waveform which represents the amount of backscattered light is produced by the receiver electronics (Figure 2.1). A time interval counter is triggered by the leading (rising) edge of both the emitted and any returning peaks observable in the waveform (Baltsavias, 1999; Höfle and Pfeifer, 2007). The range (R) to the object from the LiDAR can then be determined using the equation $R = c(t/2)$ where c is the speed of light, and t is the laser pulse's time of flight (Baltsavias, 1999).

As the laser pulse travels away from the ALS it diverges at an angle specified by the manufacturer which is usually between 0.25-1 mrad (Deems and Painter, 2006). A divergence of 0.25 mrad produces a footprint with a diameter of 25 cm on the ground at a flying height of 1000 m. If there are objects at multiple elevations within the path of the laser pulse, backscatter from all of these objects will return to the system creating peaks within the waveform (Figure 2.1) Each of these peaks (usually up to four total) then gets recorded as a discrete point to the ALS computer system (Wehr and Lohr, 1999). Allowing multiple returns from a single pulse allows the LiDAR to penetrate through holes in the canopy of trees and other vegetation to return points from the ground (Deems and Painter,

6

2006). Figure 2.1 shows a pulse that would return three pulses from within the canopy of a tree as well as a last pulse from the ground underneath. This feature is important when creating bare earth Digital Elevation Models (DEMs) because it allows the removal of trees to better characterize the underlying terrain (Axelsson, 2000).

LiDAR systems used in commercial ALSs and other products often record a digital number that represents the peak amplitude of light being backscattered for each return. This digital number is referred to as the intensity of a LiDAR return (Höfle and Pfeifer, 2007). Intensity values are dependent on several factors including: the outgoing laser power, range/atmospheric attenuation, surface characteristics of the object(s) being illuminated, and beam divergence (Kaasalainen et al., 2005). When integrated as part of an ALS the LiDAR outputs timestamped range(s) received after each emitted pulse. In most commercial ALSs, the LiDAR outputs up to 4 returns as well as the intensity of each return recorded by the LiDAR (Baltsavias, 1999; Wehr and Lohr, 1999).

The scanning subsystem of an ALS is the system that redirects the outgoing laser using a specific scanning pattern. The optics for the transmitted and received light are aligned with the scanner so that they will have the same instantaneous field of view no matter which direction the scanner is pointed (Baltsavias, 1999). Several types of scanning systems are used in commercially available ALSs including: oscillating mirror, palmer scanner, fiber scanner, and rotating polygon. Each of these scanning systems uses a different method to redirect the outgoing and incoming pulses of light creating different scanning patterns on the ground (Wehr and Lohr, 1999). The scanning subsystem in Optech's Airborne Laser Terrain Mapper (ALTM) system used for this study uses an oscillating mirror which creates a Z-shaped bidirectional pattern on the ground (Optech Inc., 2011a). During collection the scanning system outputs its precise location, recorded as an angle, to the controlling
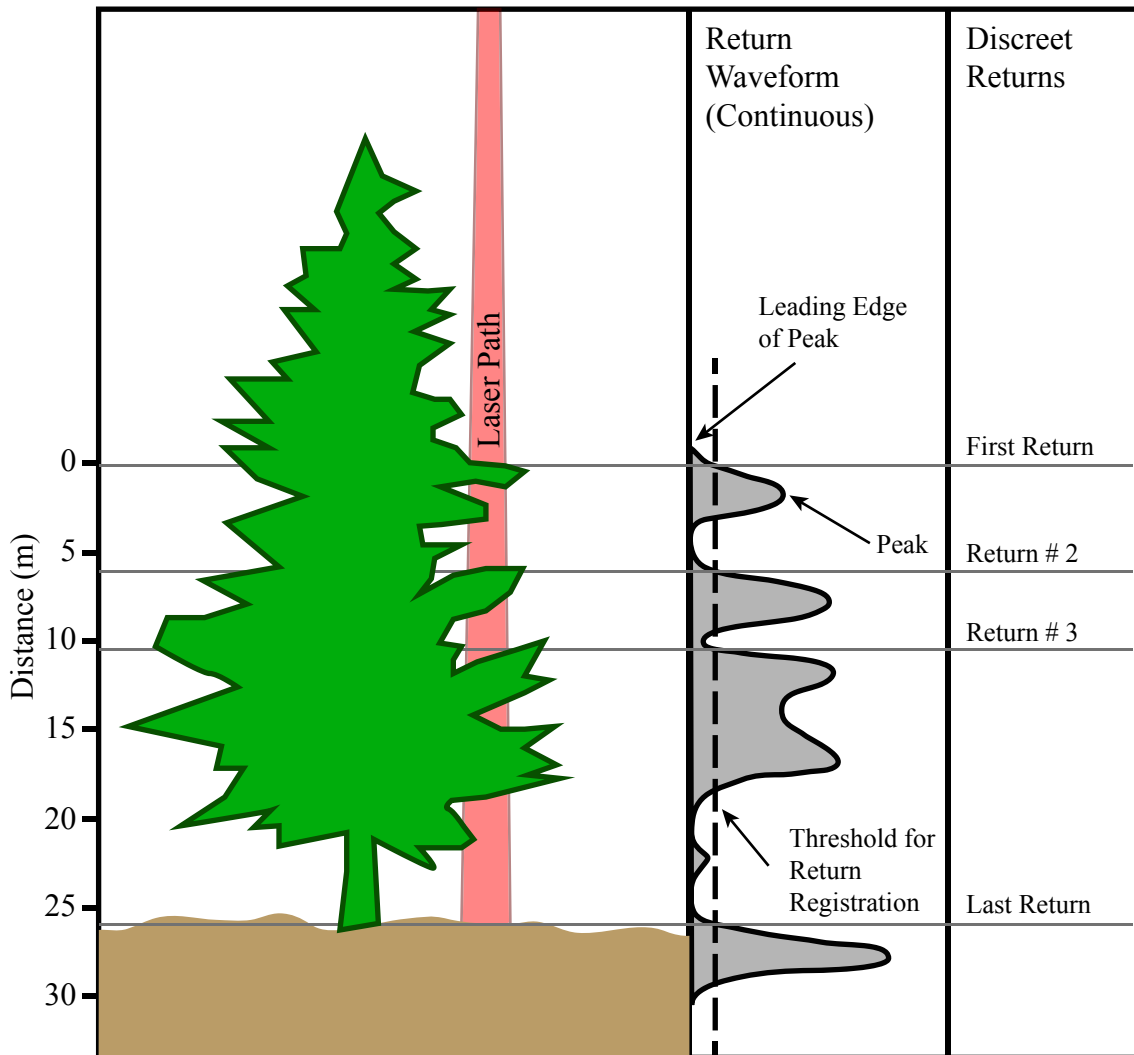
Figure 2.1: ALS pulse illumination path and return waveform. In this example portions of the pulse (red) are backscattered of objects at different heights resulting in multiple return signals. The elevation of the first three peaks as well as the last peak would be recorded. Reproduced from Deems and Painter (2006)

computer which is later used to calculate the position of the returning laser pulse during post-processing (Wehr and Lohr, 1999).

The POS subsystem of an ALS measures and records the precise position of the reference frame (usually a fixed wing aircraft) using a combination of an Inertial Measurement Unit (IMU) and a Global Positioning System (GPS) receiver (Mostafa and Hutton, 2001; Wehr and Lohr, 1999). An IMU uses accelerometers and gyroscopes to measure the attitude and velocity of the reference frame outputting the roll, pitch, yaw, and xyz velocity at up to 1000 Hz (Mostafa and Hutton, 2001). Along with the attitude of the reference frame, the position in relation to a datum is recorded using a GPS receiver at 1 Pulse Per Second (1 PPS). The IMU and GPS data are recorded during operation of the ALS and used during post processing to determine the precise location of the reference frame, for each returned pulse, relative to the World Geodetic System 1984 (WGS84) datum (Baltsavias, 1999; Wehr and Lohr, 1999).

The controlling computer controls all of the subsystems and records the values being returned from each of the subsystems along with the precise time for each piece of data. Data from an ALS needs to be post-processed once it has been collected to output the final product which is a three-dimensional point cloud (Liadsky, 2007). The first step in post processing is to differentially correct the GPS data using 1 PPS GPS data from a known basestation. With ideal GPS signal throughout a data collect accuracies of less than 5 cm can be reached with post processed GPS data (Mostafa and Hutton, 2001). The next step during post-processing is to create a best estimate of trajectory, of the reference frame, based on the corrected 1PPS GPS data, the recorded IMU data, and the measured offsets from the GPS antenna to the ALS reference point (usually the center of the scanning mechanism). The best estimate of trajectory, range data, recorded scanner angle, as well as other atmospheric and calibration corrections can then be used to calculate the position of each recorded laser pulse relative to the WGS84 datum (Wehr and Lohr, 1999).

9

2.2 Airborne Laser Scanner Sources of Uncertainty

Sources of uncertainty within ALSs have been described in detail by Baltsavias (1999); Hodgson and Bresnahan (2004); Maas (2003); Wehr and Lohr (1999) and Ussyshkin and Smith (2006). Uncertainty in ALS measurements can be grouped into two groups: 1) uncertainty within the ALS itself and 2) uncertainty caused by the target surface. All of these uncertainties affect both the vertical and horizontal (planimetric) accuracies to different extents. Vertical uncertainties are generally considered in the literature to be much smaller than the horizontal uncertainties that can occur. The uncertainties within ALS measurements, specifically for the ALTM Gemini used for this study, will be further discussed in this section.

The ranging, scanning, and POS subsystems of an ALS all have associated amounts of uncertainty that are often described within the system specifications. Uncertainties within the ranging subsystem are mostly due to the finite resolution of the time interval counter and have more effect on the vertical accuracy of an ALS than the horizontal accuracy. Overall uncertainty in the ranging subsystem is usually within ±3 cm and is unaffected by range to the target surface (Deems and Painter, 2006). The scanning subsystem shows the mostly horizontal uncertainty which is related to the finite resolution of the angular measurements recorded. The uncertainties within the scanning subsystem however are within 0.001°, or about ±2 cm on the ground which is one of the smaller sources of uncertainty (Ussyshkin and Smith, 2006).

The largest source of uncertainty in an ALS system is the POS. A POS, as described in section 2.1, uses an IMU and a GPS to create a best estimate of the trajectory of the aircraft (Mostafa and Hutton, 2001). Commercially available IMUs are capable of outputting the

10

attitude of an aircraft to within 0.005° causing a horizontal uncertainty of < 9 cm on the ground. Vertical uncertainties caused by the IMU itself are negligible (< 1 cm) and are therefore not a major influence on the error budget (Mostafa and Hutton, 2001). The largest amount of uncertainty in the POS system is the achievable positional accuracy of the GPS receiver (Ussyshkin and Smith, 2006). Advancements in GPS technology have allowed many of the sources of uncertainty to be removed, mostly through post-processing and differential corrections. Unfortunately, there are still uncertainties caused by Earth's ionosphere which cannot be removed through differential correction or post processing (Mostafa and Hutton, 2001). The uncertainty within the GPS measurements made by the POS can be between 5 cm and 30 cm depending on the number and position of satellites as well as the baseline distance to the nearest ground reference station. Uncertainty in the GPS measurements are not usually included as part of the manufacturer-specified error budget since these accuracies can change on a flight to flight basis depending upon mission planning and satellite coverage (Ussyshkin and Smith, 2006).

The type of ALS used for this study was the ALTM Gemini which is manufactured by Optech inc. of Vaughan, Ontario. The manufacturer-specified accuracy of the ALTM at the settings used for this study (shown in table 3.1) were calculated to be $< \pm 18$ cm horizontal and $< \pm 15$ cm; 1σ vertical (Optech Inc., 2011a). These accuracies do not include uncertainties introduced by the GPS measurements which can add another 5 cm to 35 cm depending on the quality of the collected GPS data. The accuracies quoted by the manufacturer as described above are easily achievable on flat homogeneous terrain but the affects of differing surface types are not included in the accuracies provided by manufacturers.

The second type of uncertainty in an ALS measurement is caused by the properties of the target surface and is often not included in a project's error budget (Deems and Painter, 2006). Uncertainties caused by the target surface are mostly related to the vertical and horizontal uncertainties caused by the ALS. The primary sources of uncertainty from the target surface are due to surface slope and vegetation on the surface (Hodgson and Bresnahan, 2004). Extreme surface slopes when combined with horizontal uncertainties of the ALS can decrease the vertical accuracy of the individual elevation measurements (Hodgson and Bresnahan, 2004). Dense vegetation near the ground on the other hand can cause the leading edge of the waveform collected by the ALS to be less pronounced causing an error in where the ALS picks the discreet point along that waveform (Hopkinson et al., 2004). The errors caused by surface characteristics are are usually ≤ 30 cm and can be minimized if the ALS survey is well planned (Hodgson and Bresnahan, 2004).

All of the types of uncertainty and error described in this section must be accounted for during the planning, collection, and processing of ALS data to produce an accurate end product. Biases in the positional accuracy caused by the GPS can be minimized between overlapping datasets with small vertical shifts to align the datasets to one another if necessary. These small adjustments improve the relative accuracy of the two datasets and can improve the absolute accuracy depending on the direction of the shift. For this study the relative accuracy of the three datasets collected was most important factor so a relative accuracy assessment was completed to assess possible errors.

2.3 Factors Influencing the Distribution and Physical Properties of Snow

The spatial distribution and physical properties of snow have been studied extensively in the past because snow has an important role in controlling the Earth's albedo and is an important source of drinking water (Elder et al., 2009b; Rees, 2006). Currently, most research is focused on determining Snow Water Equivalent (SWE) over large areas for use as input to hydrological models (Elder et al., 2009b). There is also a considerable body of literature on the processes that control the distribution of snow and their effect on SWE (Pomeroy and Gray, 1995). This section will give a brief overview of our current knowledge of the spatial distribution and physical properties of snow and how they may be affected by built-up environments.

Our current understanding of snow and how it is distributed is focused mainly within natural environments. Natural environments which have been studied in the past include the mountains, prairies, tundra, and boreal forest (Elder et al., 1991; Ho and Valeo, 2005). Several different scales of variation have also been taken into consideration which include: macro-scale, meso-scale, and micro-scale. Macro-scale encompasses variation at the 100 km to 1000 km range while meso-scale includes variation at the 1 km-10 km and micro-scale is in the 10 m to 1000 m range (McKay and Gray, 1981). Much of the current literature attempts to estimate, and describe the macro and meso-scale distribution of snow, specifically SWE. The micro-scale distribution of snow is often only used to attempt to improve models running at larger scales. All of the properties that affect the distribution of snow work at different scales depending on the environment and the property being measured. The main factors that affect the distribution of snow are described in the paragraphs below.

13

The distribution of snow in a natural environment is mainly controlled by temperature, wind, energy and moisture transfer, and the physiography of the environment including vegetation cover (McKay and Gray, 1981). In a natural environment, temperature does not directly change the distribution of snow but effects the processes that distribute snow, and how they are able to distribute snow across a region (Pomeroy and Gray, 1995). Temperature affects the crystal structure, dryness and hardness of snow as it is falling, being transported, as it settles and during melt (McKay and Gray, 1981).

Wind is one of the primary controls on the distribution and re-distribution of snow in most environments and at all scales (McKay and Gray, 1981; Pomeroy and Gray, 1995; Watson et al., 2008). The primary effect of wind is the re-distribution of snow once it has been deposited on the ground; this is when wind transports snow through one of three processes; creep, saltation, or turbulent diffusion (McKay and Gray, 1981). Global and regional wind patterns also effect distribution at regional and local scales (McKay and Gray, 1981).

Energy within a snow pack comes from three major sources, incoming solar radiation, the ground and the surrounding air mass (McKay and Gray, 1981). The primary influence on changes in depth and density of a snowpack through the winter is net radiative flux (McKay and Gray, 1981). The optical properties of snow, specifically albedo, play a big role in the net radiative flux of the snow (Warren, 1982). The surface albedo of fresh pure snow with no contaminants is usually more than 80%, meaning that 80%, of the short-wave radiation hitting the snow's surface is reflected back into the atmosphere. Lower surface albedo on the other hand allows more incident radiation to be absorbed, allowing changes in the physical properties of the snow (Warren, 1982). Heat transfer from the ground below and the air mass above the snow pack can also change the crystal structure, depth, density,

14

and mass of the snowpack (McKay and Gray, 1981).

The physical geography of the environment such as elevation, slope and aspect and land cover should be taken into consideration when characterizing the distribution of snow (McKay and Gray, 1981). Although elevation does not appear to have an immediate impact on the distribution of snow at the local or micro-scale; it does have an impact at the macro-scale for the simple reason that the higher you are the cooler the air temperature is (Pomeroy and Gray, 1995). Slope and aspect on the other hand play a big role in the distribution of snow especially at the micro-scale (10-1000m). At the micro scale, in combination with the wind, the slope of the terrain often causes snow to drift (Pomeroy and Gray, 1995). Snow drifts form on the leeward slope of the wind direction and often contain twice as much snow as the windward slope (McKay and Gray, 1981). Aspect affects the distribution of snow in two ways: 1) aspects making up the leeward side of a slope usually accumulate more snow 2) aspects receiving more energy, or facing south (in the northern hemisphere), allow faster melt (Pomeroy and Gray, 1995). Land cover, specifically vegetation, has a pronounced effect on the distribution of snow at the micro and meso-scale. Presence and density of vegetation cover can effect the amount of blowing snow that stays in an area (Watson et al., 2008). Snow is much more likely to fall to the ground due to the heavy turbulence around trees rather than in an open field where turbulence is much closer to the ground (McKay and Gray, 1981).

The factors that influence the distribution and physical properties of snow in natural environments have been described above. Built-up environments are very different from natural environments and each of the above factors could effect the distribution and phys-ical properties of snow differently as well. How these factor might change in a built-up environment are described in the following section.

2.3.1 Properties of Snow in Built-Up Environments

Research on the distribution and physical properties of snow within built up environments is sparse, limiting our understanding of how snow is distributed and what factors influence its distribution within these environments. Temperature, although not directly controlling the distribution of snow, is usually higher in built-up areas, due to the urban heat island effect (Kim, 1992). Higher temperatures will cause earlier, more rapid snowmelt and sublimation (Buttle and Xu, 1988). Wind will have the same effects that it has in a natural environment, but physical differences in the geography will have an effect on wind patterns which will effect how snow is distributed (Valeo and Ho, 2004).

Most research that has been completed on snow in built-up environments has been focused on snowmelt and runoff. The dominant cause of snowmelt is net radiative flux, which is much higher in built-up areas than in natural environments (Buttle and Xu, 1988). Net radiative flux is the total flow of radiation into or out of the snow pack determined by measuring the total ingoing and outgoing short-wave (light) and long-wave (infrared/heat) radiation within the snow pack. In a regular natural environment a snowpack would receive incoming short-wave radiation from the sun and outgoing short-wave radiation is the amount of light that is reflected away. Long wave radiation in the form of heat transfer comes from the surrounding air and ground surfaces. Enhanced net radiation of snowpacks in built-up areas is caused by proximity to buildings which cause higher air temperatures and extra sources of longwave radiation (Ho and Valeo, 2005). Another dominant control on the distribution of snow in built-up environments is the anthropogenic re-distribution and removal of snow. Snow is seen as a nuisance in built-up environments and is therefore ploughed, piled, and removed from streets, sidewalks, and parking lots (Boyd et al., 1981). This interference disturbs the snowpack and changes the distribution as well as evolution of

the snowpack. Snow that is piled and banked is often compacted and therefore has higher densities than natural snow. Disturbed snow is also often much dirtier than natural snow, which effects the albedo of the snowpack as described above(Ho and Valeo, 2005).

For the purpose of this study snow in built-up environments will be classified as either disturbed or undisturbed. Disturbed snow has been moved from its original location and piled or banked along roads and parking lots, etc. Undisturbed snow is classified as snow that has not been moved or disturbed through human interference. Undisturbed snow is found on the ground in open areas such as fields, parks and lawns. This classification is similar to the one used by Ho and Valeo (2005) who classified snow as either piled, banked, or undisturbed. Ho and Valeo (2005) found that piled and banked snow were similar in density and other properties so they have been combined for this study.

2.4   Measuring the Distribution of Snow

Traditional methods for measuring snow include: SWE/depth transects (usually $\geq$ 100 m), using snow stakes, and using groups of instruments such as snow pillows or ultrasonic sensors (Deems et al., 2006). Most measurements made to measure distribution of snow are simple point measurements made at weather stations that are sometimes hundreds of kilometers apart (Elder et al., 1991). The most common measurements made when trying to characterize the distribution of snow are depth and density, which are used to determine the SWE of the snow pack. In heterogeneous landscapes such as in mountainous regions these methods can be time-consuming, expensive, and dangerous but are still often completed to improve and validate other methods of retrieving this information (Deems et al., 2006; Deems and Painter, 2006). In built-up environments however, many

of the traditional methods are difficult at best to use because of obstacles such as traffic, buildings, roads, and private property (Matheussen and Thorolfsson, 2001). Many of the current methods are meant for estimating the macro-scale distribution of snow and not micro or meso-scale variation.

Many studies have been completed since the 1960s on the use of satellites for measuring the distribution of snow (Rees, 2006). Several methods of estimating the amount of snow on the ground have been tested using both passive and active microwave remote sensing as well as several visible and thermal instruments (Davis et al., 2008). The issue with many of these instruments is spatial resolution, which is in the order of tens of meters to tens of kilometers for many platforms. The Advanced Microwave Scanning Radiometer - Earth Observing System for example, has a footprint size of 25 km on the ground and is used for determining the SWE in large homogeneous areas but is hard to use for heterogeneous areas like mountainous or built-up environments (Chang et al., 2003). Due to the difficulties in measuring snow depth or SWE from satellite based platforms in heterogeneous areas some research has been completed on the use of airborne remote sensing, specifically LiDAR, for measuring the distribution of snow (Deems et al., 2006; Hopkinson et al., 2004; Otake, 1980).

2.5   Interaction of LiDAR with Snow Surface

Research on the optical and spectral properties of snow has been occurring for decades but there has been little research completed on the spectral response of snow in direct backscatter (Kaasalainen et al., 2006). Even less research has been performed on the spectral response of snow in direct backscatter at the wavelength of 1.064 μm, which is the

wavelength of the ALTM used in this study (Larsson et al., 2006). Previous work completed on the spectral response of snow has found that the reflectivity at 1.064 μm is dependent on grain size which can be seen in figure 2.2 (Zibordi et al., 1996). The Bidirectional Reflection Distribution Function (BRDF) of snow at the wavelength of 1.064 μm is similar to the BRDF at 0.532 μm (Aoki et al., 2000) which has a high reflectivity in direct backscatter (Kaasalainen et al., 2006). Kaasalainen et al. (2003) also proved the existence of a "hot-spot" around 0° phase angle in the visible spectra, where reflectance amplitude was much higher than greater phase angles, regardless of incident angle. All of the above discoveries provide a reasonable case for the assumption that direct backscatter from a 1.064 μm laser exhibits similar characteristics of a laser at 0.532 μm, but with a higher dependence of grain size.

Impurities in snow within built-up environments can be categorized into two distinct categories: impurities introduced as the snow forms, and impurities introduced to the snow pack post accumulation. Impurities introduced as the snow forms have been studied along with their effect on the spectral albedo of snow (Warren, 1982). For impurities such as soot and volcanic ash, which are often present in the atmosphere, the effect on the spectral albedo of snow at wavelengths $\geq$ 0.9 μm were determined to be negligible (Warren, 1982). Impurities introduced into the snow pack post accumulation such as road salt, sand, and brake dust will all have an effect on the albedo of snow (Ho and Valeo, 2005), but these effects are unknown at 1.064 μm. For this study it is assumed that even with impurities, snowpack in built-up environments will have a reflectance greater than the 10% needed for an ALTM to record a range (Optech Inc., 2011a).

A source of uncertainty that was not mentioned in section 2.2 is the transmission of snow at the wavelength of 1.064 μm. To date little research has been completed on the

19
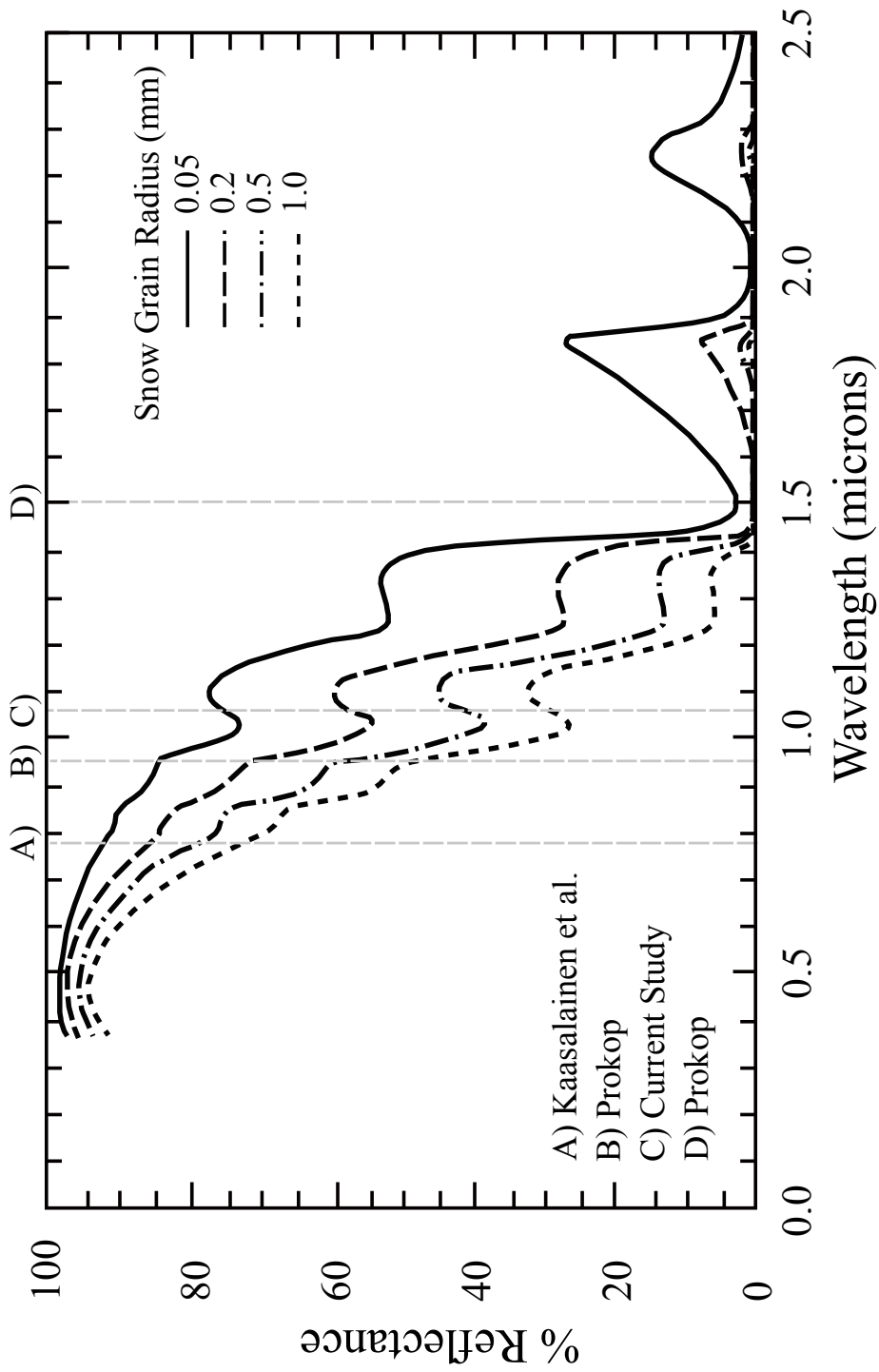
Figure 2.2: Typical reflectance spectra of snow for 4 different grain sizes. Vertical lines A to D represent different wavelengths of terrestrial and airborne ALSs including the wavelength used for this study (1.064 μm). Reproduced from Warren and Wiscombe (1980) and Dozier et al. (2009)

optical transmission of snow. Studies that have been completed focus on 0.350 μm to 0.9 μm wavelengths of the electromagnetic spectrum (Beaglehole et al., 1998). Deems and Painter (2006) explain that it is reasonable to assume that 97% of the scattering and absorption happens within the top 1 cm of the snow pack regardless of the snow physical properties. To support their argument, Deems and Painter (2006) explain that at 0.9 μm 97% of backscatter happens within the top 2 cm of the snow pack (Beaglehole et al., 1998) and that at 1.064 μm the same attenuation of radiation will occurr at a shallower depth (< 1 cm). This assumption is backed up by a study completed by Prokop (2008) in which they used Terrestrial Laser Scanners (TLSs) at 0.95 μm and 1.5 μm to compare backscatter from a rough snow surface and reflective foil at the same distance. The results from the study by Prokop (2008) proved that ranges were being backscattered from depths of < 1 cm.

2.6 Using LiDAR for Measuring Snow

Several studies have been completed in the past 10 years that have used airborne, terrestrial and mobile LiDAR systems to measure the physical properties and depth of snow (Deems et al., 2006; Hopkinson et al., 2004; Kaasalainen et al., 2011; Prokop, 2008). Most of the focus in recent years has been on the use of LiDAR for measuring the amount of snow in mountainous environments because it is otherwise difficult to characterize snow in such rugged areas (Grünewald et al., 2010). The basic methodology is very similar between the three types of LiDAR systems used for measuring snow. Scans are completed before and after snowfall, then the elevations are differenced to estimate snow depth. Figure 2.2 shows the spectral reflectance of snow along with vertical lines at wavelengths that have been used for measuring snow.This section summarizes previous work that has been com-

pleted on the use of LiDAR for measuring snow, and how these methods can be applied in this study.

Most of the research completed on the use of LiDAR for measuring snow has been completed using TLSs. Kaasalainen et al. (2008) used a 0.785 μm TLS at close range (< 30 m) to detect changes in the snow pack throughout the winter of 2007-2008. Both the range and calibrated intensity values from the TLS were used in their study. The range measurements from the LiDAR were converted to elevations which were differenced between scans to estimate the difference in snow depth, while the intensities were used to estimate grain size and surface wetness. Kaasalainen et al. (2008) determined that the TLS was capable of accurately monitoring changes in snow depth but concluded that further research is needed before useful information can be obtained from the intensity values. Egli et al. (2011), Grünewald et al. (2010), Prokop (2008), and Prokop et al. (2008) all used TLSs with wavelengths between 0.95 μm and 1.5 μm to estimate the depth of snow in mountainous environments. Prokop (2008) and Prokop et al. (2008) were able to measure the depth of snow to within $\pm$10 cm for ranges < 800 m in their study but found that the effects of terrain and laser footprint size decreased this accuracy over 800 m. They also found that the TLS running at a wavelength of 1.5 μm had limited success in measuring snow cover due to poor reflectance at that wavelength (seen in figure 2.2). Egli et al. (2011) and Grünewald et al. (2010) measured the spatio-temporal evolution of snow distributions using several TLS scans in mountain catchments but neither study published the accuracy of their TLS measurements compared to ground based methods. Overall several studies have shown that TLSs are capable of measuring snow depths to within $\pm$10 cm of the actual depth, but applying these measurements to large built-up environments would be impractical. TLSs are ground based instruments that are usually mounted between 1 m

and 3 m above the ground and scan horizontally in a specific direction which can cause undesirable shadowing behind obstacles such as buildings (Prokop et al., 2008). This makes them ideal for scanning snow on mountainsides but limits their use for measuring snow in built-up environments.

Kaasalainen et al. (2011) used a snowmobile-mounted mobile laser scanner, running at a wavelength of 0.785 μm, to scan an 11.5-km transect of snow in Sodankylä, Finland. The primary focus of their study was to determine if mobile laser scanning could be used to measure snow surface roughness in their study. Kaasalainen et al. (2011) were able to determine snow surface roughness with accuracies < 1 cm, tested against more than 200 validation transects. A qualitative assessment was also completed to determine the feasibility of using mobile laser scanners for snow depth change detection which showed promising results. Unfortunately, like the TLS systems mobile laser scanners are often < 3 m above the ground limiting the coverage area in built-up environments due to shadowing at high incidence angles. Mobile laser scanners are also often limited to ranges between 100 m and 200 m because of eye safety regulations (Optech Inc., 2011b).

ALS has been used in studies by Deems et al. (2006); Hopkinson et al. (2004) and Moreno Baños et al. (2011) for determining the distribution of snow over larger areas. Hopkinson et al. (2004) and Moreno Baños et al. (2011) both completed accuracy assessments to validate the use of ALSs under forest canopy and in mountainous terrain respectively. Hopkinson et al. (2004) found a statistically significant relationship between ground-measured and LiDAR-estimated snow depths which was strongest in pure conifer plots, when compared to other types of forest cover. They also found that there was an underestimation of snow depths due to understory vegetation in some of their study sites. In general the distributions found by Hopkinson et al. (2004) were found to qualitatively very

similar to observations previous observations of the distribution of snow. Moreno Baños et al. (2011) were unable to validate their LiDAR-estimated snow depths against ground measurements due to large uncertainties in the ground measurements. Validation for the study by Moreno Baños et al. (2011) was therefore completed by digitizing areas with no snow (assumed to be 0 cm depth) from orthophotos of the study site and calculating the RMSE from these areas against the LiDAR difference map. RMSE in this study varied between 17 cm for slopes $< 10°$ up to 130 cm for slopes between 50° and 60°. The average RMSE for slopes between 0° and 60° measured by Moreno Baños et al. (2011) was 43 cm.

Deems and Painter (2006) compiled a list of the theoretical accuracies and error sources that could occur when using an ALS for measuring snow depths. These uncertainties are described in detail in section 2.2. Deems et al. (2006) used an ALS to measure snow depths in a mountain environment and then used the acquired snow depths to describe the fractal distribution of snow in this environment. For validation of the snow depth data they referenced the work completed by Deems and Painter (2006) and Hopkinson et al. (2004). Built-up environments are very different from the natural environment and as described in section 2.3.1, so is the snow within these environments. For this reason, previous validations of ALS data for measuring snow depth do not apply in built-up environments.

This review of methods used for retrieving snow depths with LiDAR shows that ALSs are the best choice in an built-up environment. Both TLSs and mobile mappers use horizontal measurements which are affected by shadowing making them impractical for measuring snow in this environment. It is also shown that a wavelength between 0.5 μm and 1.1 μm would be best since these wavelengths have much higher reflectance values on snow than wavelengths > 1.1 μm. 1.064 μm is therefore an appropriate wavelength for collecting snow depth data. It can be expected based on the studies reviewed in this chapter that an ALS

24

will be able to estimate the depth of the snow pack but validation should be completed to verify the measurements.

Chapter 3

Methodology

3.1 Description of Study Site

The study site for this thesis is the town of Uxbridge Ontario, which is located approximately 60 km northeast of Toronto, Ontario, Canada (figure 3.1). This site was chosen because it is between two of Optech Incorporated's primary ALTM calibration sites allowing the collection of several LiDAR datasets with minimal cost. Uxbridge Ontario is also easily accessible to the author and has a variety of land cover types ranging from built-up to rural within a small area. The study area boundary (red outline in figure 3.1) is the intersection area of the three LiDAR datasets that were collected for this study. Detailed maps of each individual study site are included in the appendix.

The study site receives an annual average of 94 cm of snowfall between the beginning of December and the end of February each year, over an average of 32 days with measurable snowfall. The average temperature in the study area for the same time period is -3.9°C (Environment Canada, 2011). Although there is an average of 94 cm of snowfall throughout

the winter season, snow on the ground is rarely this deep because of compaction and melting throughout the season (McKay and Gray, 1981).

3.2 Data Collection

Data collection for this project was completed over two winter seasons starting in the fall of 2009. Three ALS flights were completed, the first was in the fall before the onset of snow accumulation, the second and third were collected during accumulation periods. The two winter datasets were collected near the beginning of February which was close to peak accumulation for the study area. Manually measured snow depths were also collected within 24 hours of each of the winter ALS flights. This section will describe the planning and implementation of the ALS surveys as well as the manually collected snow depth measurements.

3.2.1 Airborne Data Collection

Before airborne data collection could be completed a survey plan was created which specified the parameters needed to collect data at the required point density. Flight planning was completed with Optech's ALTM-Nav Planner software which allows optimization of flight parameters to suit the needs of the survey. A point density of 4 points per meter squared was selected as an optimal point density for the fall flight, while 2 points per meter squared was selected for the two winter flights. A higher point density was selected for the fall flight to increase the possibility of receiving returns from the ground even through areas with more dense tree cover. It was important to have more ground points in the fall data to ensure accuracy in the bare ground DEM. Once flight plans had been created they were given to Optech's flight department to be flown at their convenience.
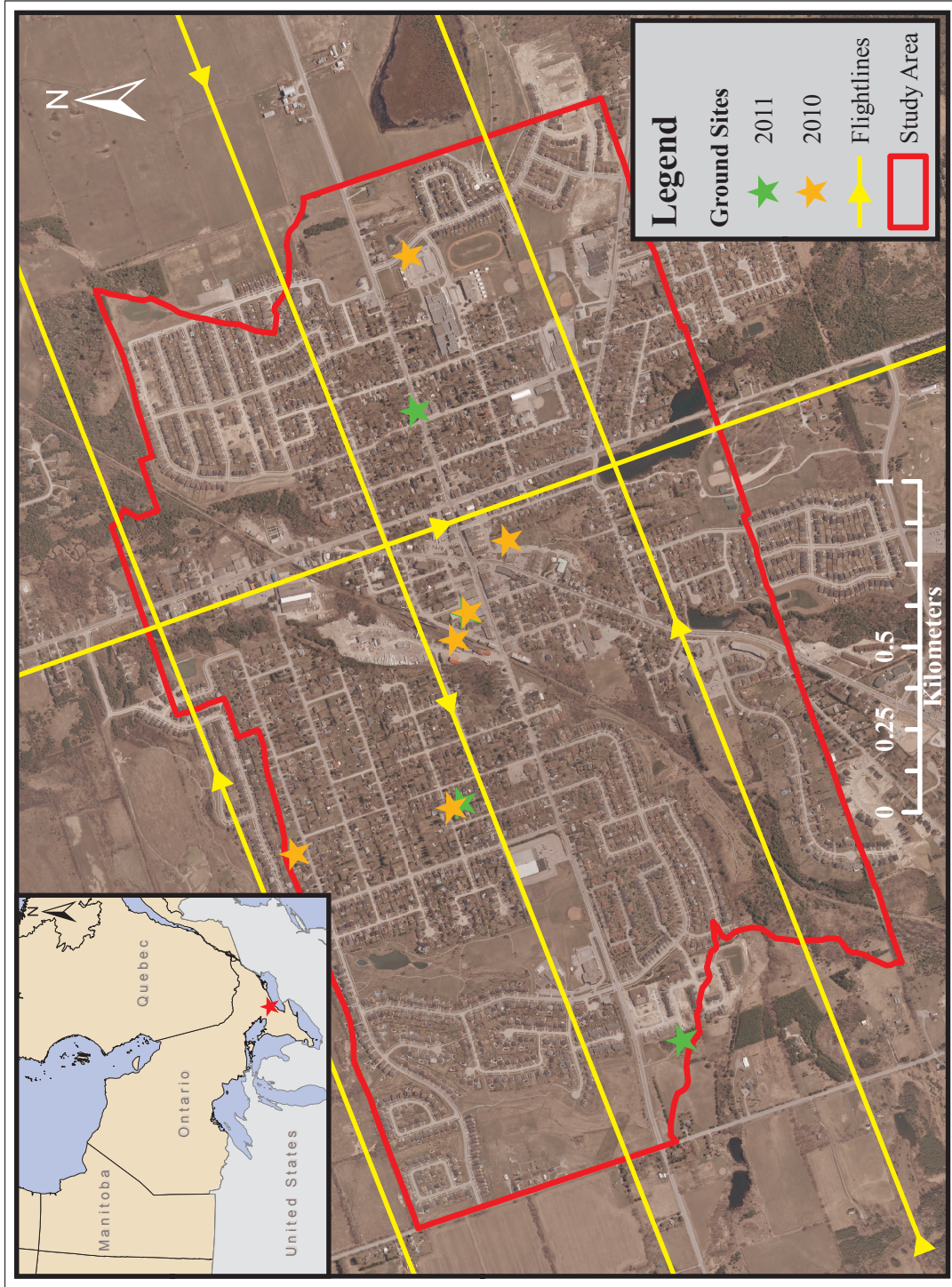
Figure 3.1: Overview map of the study area (Uxbridge, ON) showing the study area boundary in red, flightlines from the 2 winter flights in yellow, and the 2010 and 2011 study sites as orange and green stars respectively.(J D Barnes Limited, 2008)

The first ALS flight was completed on October 25th, 2009 which was mostly cloudy and cool, with no snow cover present. This was an ideal date for collection of the fall ALS data because there were very few leaves left on trees allowing the ALS to penetrate the canopy and collect more points on the ground. The fall ALS survey consisted of 9 flightlines, 5 E-W and 4 N-S, containing 49,635,154 points within the study area boundaries. The survey parameters used for each flight were selected during the flight planning process and are listed in table 3.1.

The second of the three flights was flown on January 30th, 2010 which was the approximate peak accumulation of snow cover for the 2010 season. This flight consisted of 4 flightlines, 3 E-W and 1 N-S, collecting 15,080,779 points within the study area. The N-S flightline as well as the middle E-W flightline were collected over major roads to be used to ensure alignment between scans during the accuracy assessment. The scan angle used for this flight was different than the other two flights, due to operator error, which slightly changed the point density making the 2010 dataset the least dense of the three datasets.

The second winter flight was completed on February 3rd, 2011, just over a year after the first winter flight. Although not initially planned for, this flight was completed because there was a much deeper snow pack present in 2011 than the previous winter. The plan used for this flight was the same as the second flight with 3 E-W lines and 1 N-S line being collected. The correct scan angle was used for this flight allowing a higher point density with 18,101,907 points being collected within the study area polygon.

Table 3.1: Survey parameters used during ALS flights

	October 25th 2009 (No snow present)	January 30th 2010 (Snow Present)	February 3rd 2011 (Snow present)
PRF (kHz)	100	100	100
Scan rate (Hz)	50	40	40
Scan angle (◦)	20	25	20
Altitude (m)	800	1000	1000
Speed (m s^{-1})	60	60	60
Planned Density (PPM^2)	4	2	2
Flightlines	9	4	4

3.2.2 Ground Data Collection

Snow depth measurements were made within 24 hours of each of the flights over snow, using ground based survey methods. An automated GPS snow depth probe was used for collection of the 2010 dataset but was unavailable for the 2011 season. Sites for ground based data collection were selected based on accessibility, snow cover type, and land cover classification. For the purpose of site selection, snow types were classed into two categories: disturbed and undisturbed. Selected sites ranged from heavily built-up areas to the suburban/rural boundary and an attempt was made to survey at least one of each snow type in both suburban and rural land classes. At each site descriptive notes were taken, and a map was drawn recording the location of each transect with relation to surrounding objects. The following two sections describe the two methods used to measure snow depths across the study site.

3.2.2.1 2010 Data: Automatic Depth Probe Sampling Method

The 2010 ALS flight was completed in the late afternoon on January 30th which delayed ground collection until the next morning. Temperatures through the night were between

-8 °C and -10 °C with no precipitation and low wind. Collection of snow depths using the automated GPS depth probe began at 09:00 on January 31st.

The automated GPS depth probe is an instrument developed by Snow-Hydro which uses a magnetostrictive position sensor to determine the position of a magnet along a steel shaft. The magnet is attached to a basket which sits on top of the snow as the shaft penetrates through the snow pack to the ground (figure 5.4). Once the probe reaches the ground the user pushes a button and a voltage, which is converted to snow depth, is automatically logged to a data logger in a backpack worn by the user. A geographic coordinate is also recorded for each snow depth using a GPS that is attached to the backpack. The automated GPS depth probe is capable of measuring snow depths much quicker than the manual method but the geographic coordinates of the points have a quoted accuracy of ±3 m adding uncertainty to the location of each measurement.

The first and last step at each of the sites was to test the automated GPS depth probe by taking a measurement at the minimum and maximum depths the probe is capable of. The testing process ensures that there is no change in the values the sensor is returning throughout data collection. Once the instrument was tested several perpendicular transects were collected at each site to capture the variability of snow depths within that site. Measurements along a transect were completed approximately every 0.5 m, a distance chosen to capture the variability of snowbanks and piles. Ground data collection came to an end at 14:00 due to heavy snowfall which would bias snow depth probe measurements. All measurements from the depth probe were downloaded to a PC for further processing at the end of the day.

3.2.2.2 2011 Data: Manual Depth Probe Sampling Method

As with the ALS survey from the previous year the survey on February 3rd, 2011 was completed in the late afternoon which delayed the collection of ground data until the next morning. Temperatures monitored through the night were between -5 °C and -7 °C with a light wind and no precipitation. Snow depth measurements started at 07:00 on February 4th, 2011.

Manual depth measurements were collected using a snow depth probe marked at 1 in intervals, a 30 m tape measure, a Trimble GPS and a voice recorder. A snow depth probe with imperial markings was the only probe available at the time, but measurements were made to the nearest 0.25 in which is close to the 0.5 cm of possible accuracy using a metric probe. For each transect the tape measure was first extended along the length of the transect in a straight line. The GPS was then used to collect and average more than 50 points at each end of the tape measure to mark the beginning and end of the transect. Next the snow depth probe was used to measure snow depths at 0.5 m intervals along the tape measure. As each point along the transect was measured, the depth was spoken into the voice recorder to later be transcribed in the office. This entire process was completed for each transect in every study site visited that day. Measurements were also taken at each site to locate the beginning and end of each transect from permanent objects such as buildings for further reference when digitizing the transect locations.

3.3 Data Pre-processing

Before any of the data could be classified or analyzed, several steps were taken to prepare each of the datasets for further processing. The ALS collects two different datasets, the

range data and the trajectory (POS) data. The range data includes all of the range data collected by the ALS as well as the angle the scanning mirror was pointing for each range measurement. The trajectory data contains the heading attitude, and velocity of the aircraft as recorded by the POS subsystem described in section 2.1. Before any useful geographic information can be obtained from these data they must first be combined along with some system specific parameters to georeference each point collected by the ALS. The final outputs from this process are industry standard Laser files (LAS files) which contain millions of georeferenced points for each flightline of ALS data collected. All of the above steps were completed by Optech Inc. shortly after each flight and the LAS files were obtained for further processing.

The first step after receiving the LAS files was to spatially crop each one to the study area to reduce the file size of each flightline of data. To do this, outlines were made of each of the collected flightlines using a tool called LASboundary, from the LAStools collection of software. Next, every outline from each flight was loaded into ESRI's ArcGIS software and the union, then dissolve tools were used to create an outline of all flightlines for each flight. The intersect tool was used to determine the area that was covered by all three flights. The outline created in the above steps was used as the final study area outline for this thesis. The LAStools LASclip software removed all points that were not within study area preparing the LAS files files for filtering and DEM creation.

The data from the automated GPS snow depth probe were downloaded as an ASCII text file from the data logger shortly after the data was collected. The text file was loaded into a spreadsheet application and compared with notes to check for errors or inconsistencies, of which there were none. To save space on the data logger the latitude and longitude, when recorded on the automatic snow depth probe, have decimals trimmed from the end. Integer

values representing the degrees, minutes and decimal seconds which were included in the text file were used to recalculate the latitude and longitude values giving more precision to each recorded location. All snow depth values were then imported into ArcGIS as XY points and were exported as shapefiles to be used later in the accuracy assessment.

The first step before processing the manually collected ground data was to transcribe all of the recorded snow depths and other information from the voice recorder to digital files. Recorded depths were transcribed to a spreadsheet then converted from inches to meters to match the ALS data. The recorded GPS points were then loaded into ArcGIS as XY points. Small adjustments were made to the positions of each end coordinate to ensure that each set of points represented a vector the same length as the transect it represented. Measurements taken at each field site were used to manually verify the location of each transect. Coordinates for each point, along each transect, were then calculated based on the starting coordinate and the gradient of the vector representing that transect. Once the coordinates for each point had been calculated all of the ground based measurements were brought into ArcGIS as XY points and saved as shapefiles to be used in the accuracy assessment.

3.4 Classification of Airborne Laser Scanner Data

A DEM is a raster representation of the elevation of the ground for a specific area. Digital Surface Models (DSMs) in contrast to DEMs are a raster representation of the elevation of the surface of a specified area including all objects on and above the ground. DEMs represent the bare ground surface with all other objects such as trees and buildings removed. For the purpose of this study DEMs are the appropriate choice since differencing

elevations of DSMs would produce a very non-uniform result since objects above the ground such as trees are not static from year to year. The DEMs in this study represent the ground surface for the fall 2009 flight and the snow surface for the 2010 and 2011 winter flights. Before DEMs could be created all of the LiDAR returns had to classified as either ground or non-ground points so that objects above the ground surface could be ignored during DEM creation.

Raw LiDAR data include all points from all returns that were collected by the ALS during the flight. This includes returns from trees, power lines, buildings, etc. which typically create a very variable DSM that is unrepresentative of the snow or ground surface elevation. To correct for the effects of these non-surface elevation returns, the ALS was first classified to filter out high, low, and isolated points. A ground classification algorithm must then be applied to classify each point as either ground or unclassified allowing the use of only ground points for further analysis. This allows the creation of DEMs which contain only ground/snow surface elevations without other objects that would be present in a DSM. A final classification is then run on the remaining unclassified points to determine which points belong to buildings. The building points are used to mask buildings out of the final snow depth maps. The above classification steps are described in detail in the following paragraphs.

High, low, and isolated points can all be described as erroneous points in the data that are clearly located either above other objects or below the ground. These points can be caused by interferences such as clouds, haze, or even birds and must be removed before the ground classification algorithm is run so they are not mistaken as true ground points. Erroneous points, especially ones below the surface, can cause errors in the ground classification because the algorithm used picks the lowest points as seed points before classifying other

points. Before classification started, every point in each of the LAS files was classified as LAS file class 1, or unclassified. A low points filter was then run using Terrasolid's, Terrascan software on each of the flightlines from each flight. The low points filter moved any groups of 10 or fewer points, that were more than 0.5 m lower than the average of all other points within a 5 m horizontal distance, to the LAS file class 7 or isolated points. Terrascan's isolated points filter was then used to classify any points that had less than 10 other points within a 5 m XYZ search radius to class 7 as well. Once the isolated and low points had been removed the ground classification could be run on the points remaining unclassified.

In a comparison of ground classification algorithms by Meng et al. (2009), and expanded on by Meng et al. (2010) the ground classification algorithm written by Axelsson (2000) consistently outperformed 8 other algorithms. The adaptive Triangular Irregular Network (TIN) classification created by Axelsson (2000) has been implemented as the ground classification algorithm in Terrasolid's Terrascan software package. This algorithm iteratively adds points to a TIN based on a user defined maximum distance and angle of each point compared to the existing surface. The algorithm does this by first finding low points, or seed points, within each cell of a grid which has a cell size chosen by the user. The grid size for selecting the original seed points should be bigger than the largest expected building in the scene to ensure that at least one actual ground point is present in each grid cell. Once the seed points have been selected a TIN is created from the seed points and each iteration adds one candidate point, if there are any, to each facet of the TIN. This algorithm iterates until there are no more candidate points that are below the maximum iteration angle and distance(Axelsson, 2000).
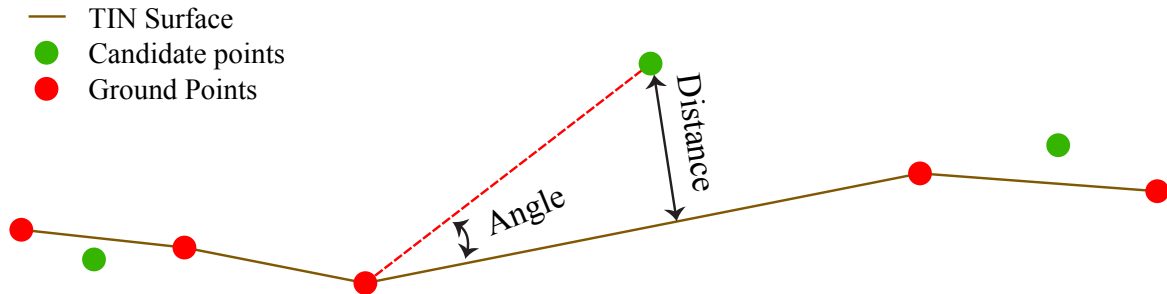
Figure 3.2: Candidate points are classified as ground based on their angle and distance from the TIN. If either of these exceed the user defined maximum they will remain unclassified.

For this study a maximum building size of 90 m was used as the grid size for selecting initial ground points. The maximum terrain angle used was 80° and the maximum iteration angle and iteration distance were 6° and 1.4 m respectively. A maximum building size of 90 m was selected because there are no buildings larger than 90 m within the study area. Setting the largest building to 90 m sets the initial grid size for selecting seed points to a 90 m by 90 m grid meaning every cell should contain at least one actual ground point. The maximum terrain angle was set high for this study to allow the inclusion of very steep snowbanks and snow piles. This also helped to include points on any terraces that were located in the more built-up areas. Iteration angles between 4° and 10° are suggested by Axelsson (2000), 4° being for very flat terrain and 10° in very hilly to mountainous terrain. An iteration angle of 6° was chosen for this study site because most of the study site is relatively flat or rolling with some areas of moderate slope. Several iteration distances were tested with a visual inspection and comparison after each test. The best results were from an iteration distance of 1.4 m which is slightly less than the default value of 1.5 m for the filter.

Once the ground classification algorithm had been run the final step was to classify the buildings within each of the ALS flightlines. The purpose of classifying buildings was to create a building mask for each of the DEMs to reduce errors in the final snow depth map around buildings. This process was completed with the 'Classify Buildings' tool in Terrascan which looks for planar surfaces that are above the already classified ground points.

All of the above classification methods were applied to each individual ALS flightline resulting in several files for each flight with each point classified into 1 of 4 classes: isolated points , ground, building, or unclassified. To make the entire dataset more manageable all of the ground points from each flight were merged into a single file, resulting in one file of only ground points for each flight. After being merged the data from all three flights were ready to be used for creating high resolution DEMs.

3.5   Creation of Digital Elevation Models

Before the ALS datasets could be used to estimate snow depth, high resolution DEMs needed to be created for each of the flights. This was done using a tool called LAS2dem from the LASTools software package. LAS2dem first creates a temporary TIN of the entire study area then uses simple linear interpolation to determine the value for each cell from the TIN. The value given to each cell in the output DEM is the value of the TIN at the center of that cell. The DEMs created from the three LiDAR flights were created at 0.5 m resolution which is the same as the sampling interval used in the manual depth measurements. Any triangles in the TIN that contained edges that were longer than 20 m were considered to have no data because the resolution of the LiDAR in these areas is

well below the resolution needed for capturing snow banks and drifts etc. Setting a 20 m cutoff value removed many areas where false values would have been found due to poor resolution such as building footprints and water bodies. A building mask, described in the next section, also helped in preventing false values around the edges of buildings in the final snow depth map

3.6   Assessing the Relative Accuracy of the LiDAR Datasets

To determine the overall accuracy of the three different LiDAR scenes relative to one another an accuracy assessment was completed on two main roads within the study area. Major roads were chosen for this accuracy assessment because they are snow-free year round and should be at the same elevation in all three ALS DEMs. ArcGIS was used to create two transects containing over 9100 points, spaced at 1 m, along the major N-S and E-W roads (yellow lines in Figure: 3.3). Next, the elevation value from each of the three DEMs was added to each of the points using the 'Extract Values to Points' tool in the Spatial Analyst toolbox of ArcGIS. This created a table where the elevations for all three flights were side by side for comparison. A spreadsheet application was then used to calculate the RMSE, MAE, and mean bias of each of the winter flights compared to the fall flight.

3.7   Creation of Buildings Mask

Buildings pose a particular problem to the creation of accurate snow depth maps because they can cause large errors. These errors occur if a building is not fully removed from one

of the DEMs, or the ALS doesn't measure the exact edge of a building. ALSs data has an irregular point spacing which means that no two flights will be exactly the same with respect to coverage. Building edges therefore can seem to be in slightly different locations from flight to flight since LiDAR pulses do not always hit the exact edge of a building which can create elevation errors up to several meters. A more detailed description of this type of error can be found in section 5.4.2, specifically figure 5.2. To overcome this issue, a building mask was created using the three combined LiDAR datasets to remove all of the
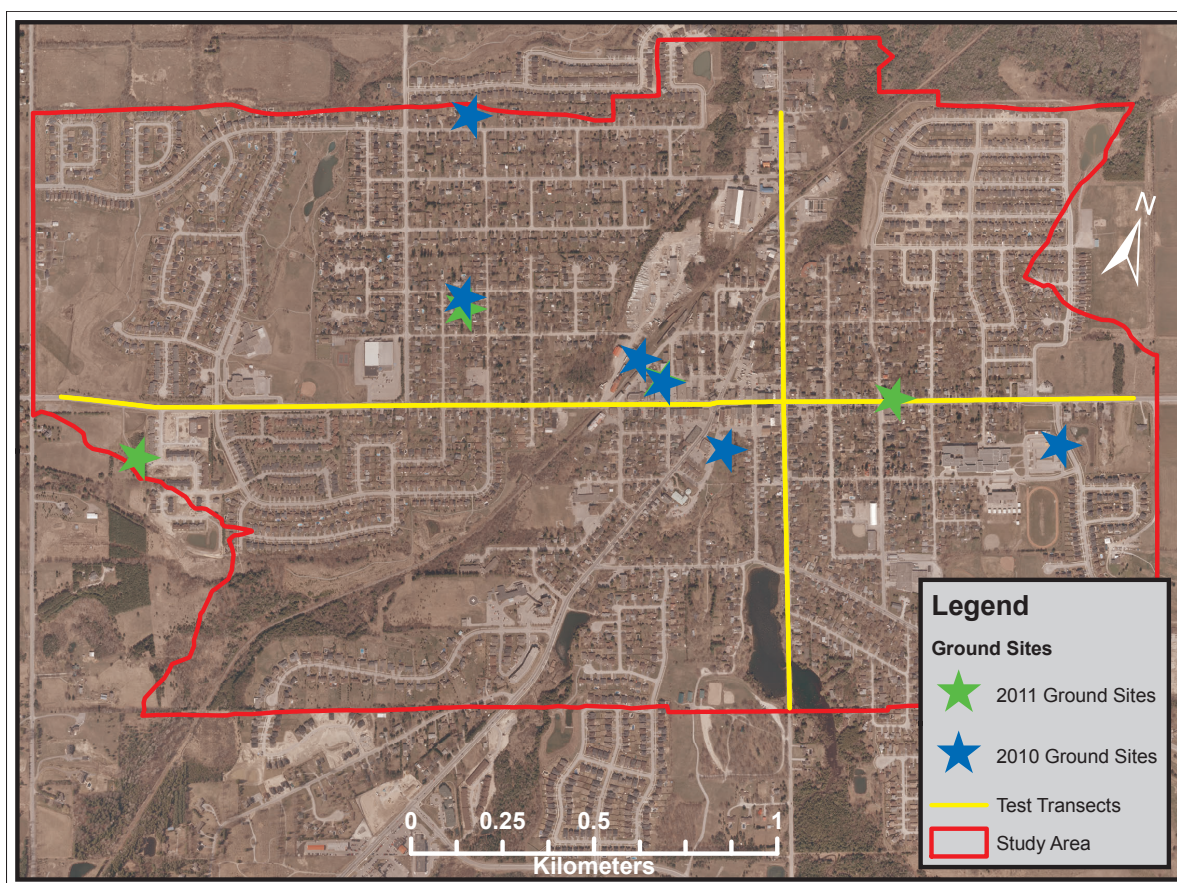
Figure 3.3: This map shows the location of the ground based measurement sites in blue and green as well as the two transects used for the relative accuracy assessment in yellow.(J D Barnes Limited, 2008)

40

building footprints from the DEMs before the snow depths were calculated.

To create the building masks all of the points classified as buildings from the three ALS flights were combined into one LAS file. The buildings LAS file was then converted to a DEM using the same LAS2dem tool used for the ground DEMs, but with a maximum triangle edge of 2 m, so buildings more than 2 m from each other would not be appear attached. The resulting DEM was then turned into a binary raster and the 'Boundary Clean' tool in ArcGIS was used to smooth out the edges of each building. This binary layer was then used in a conditional statement to ensure that all buildings were set to NoData in each DEM.

Another use for the classified buildings that was briefly explored was determining the amount of snow on building roofs. The possibility and issues around calculating this valuable information will be discussed in more detail in the discussion section.

3.8   Creation of Estimated Snow Depth Maps

The estimated snow depth maps for the two winter flights were created using the ArcGIS Spatial Analyst extension's 'Raster Calculator'. The raster calculator was used to subtract the fall DEM from each of the winter DEMs resulting in two rasters datasets containing the difference in elevation between the fall and winter for each 0.5 m cell. The difference in elevation between the fall and the winter is considered the estimated depth of the snow pack which is the final product of this study.

3.9 Assessing the Accuracy of the LiDAR Estimated-Depths

An accuracy assessment of the ALS derived snow depths was completed using the ground points created in sections 3.2.2.1 and 3.2.2.2 and the same tools used for the relative accuracy assessment in section 3.6. For each of the winter flights, the extract values to points tool was used to add the ALS derived snow depths to its corresponding ground point. This resulted in a table for each flight containing both the measured and estimate snow depths. Spreadsheet software was then used to determine the RMSE between the measured and estimated points as well as computing descriptive statistics and plotting the data by transect, site, and flight.

Chapter 4

Results

This chapter presents the results of the the analyses described in chapter 3 above. First the results of the relative accuracy assessment completed in section 3.6 will be presented, followed by maps and a description of the snow depth estimates created by the LiDAR processing methods. The ground-measured and LiDAR-estimated snow depths are then presented and compared. Lastly, an accuracy assessment is presented for the 2010 and 2011 datasets respectively including a comparison of the two datasets as a whole.

4.1 Relative accuracy of ALS datasets

The accuracy of the snow accumulation DEMs relative to the bare earth DEM was determined using the methods described in section 3.6. Table 4.1 summarizes statistics from all of the points created along the two bare road transects used for the accuracy assessment. Statistics were very similar for all three DEMs having averages within 2 cm of each other. The statistics shown in table 4.2 compare the individual accumulation DEMs to the bare-earth DEM. The RMSE and MAE show that the relative amount of error between

the three datasets is ≤5 cm across the entire study area. Table 4.2 also shows that there is negligible bias between any of the datasets. Results from the relative accuracy assessment demonstrate that the three DEMs are aligned to allow accurate snow depth estimates to be calculated.

Table 4.1: Descriptive statistics of points along the two test transects, for each of the DEMs.

Flight	Oct 2009	Jan 2010	Feb 2011
Mean (m)	244.27	244.25	244.26
Min (m)	228.73	228.69	228.71
Max (m)	276.57	276.57	276.57
Std.dev (m)	12.99	13.00	12.99
Number	5878	5878	5878

Table 4.2: Statistics showing the relative accuracy of the two snow accumulation DEMs compared to the bare Earth DEM along the two snow-free test transects.

Flight	Jan-10	Feb-11
RMSE (m)	0.05	0.04
MAE (m)	-0.02	-0.01
Mean Bias (m)	0.00	0.00

4.2   LiDAR-Estimated Snow Depth Maps

After all of the LiDAR processing steps were completed (see sections 3.3–3.5), the final output was two 0.5 m resolution raster datasets containing estimated snow depths, across the entire study area. Figures 4.1 and 4.2 show the two estimated snow depth maps as well as the ground data sites for each of the collection dates. For each of the maps, black cells indicate areas where the estimated depth is expected to be zero. Cells in black were

classified based on values within the RMSE of each DEM, determined by the relative accuracy assessment described in sections 3.6 and 4.1. Cells with negative depths are marked in red, while cells where snow depths were estimated to be above 2 m are yellow. The two different shades of blue indicate cells where snow depth estimates are within the expected range. Tables 4.3 and 4.4 show the number and percentage of cells contained in each class on the two snow depth maps.

In the 2010 estimated snow depth map, 55% of the study area is covered in a minimum of 5 cm of snow while 33% of the estimated values are snow free (within the range of uncertainty -5–5cm). More than 11% of the estimated snow depths were negative values less than -5 cm and were erroneous values. Reasons for these errors are discussed in detail in section 5.4. As can be seen in figure 4.1, most of the cells that are near or below zero (red and black) can be seen on roads and paved areas. Another area with noticeable erroneous values is directly south-east of site 2010D, which is the location of a large pond. There was also a considerable number of cells with uncertain measurements in large open areas throughout the study area. With only 0.14% of the snow depth values greater than 1 m there are no noticeable areas on the map where these depths are present, but a closer inspection shows that these values are mostly located around building edges and in heavily forested areas. These errors are described in more detail in section 5.4 as well as figure 5.3.

In the 2011 estimated snow depth map, more than 83% of the cells had an estimated snow depth of 5 cm or more. Slightly more than 9% of the cells had an estimated value within the range of uncertainty which were ±4 cm of zero, or the RMSE for the 2011 dataset. About 4% of the cells had erroneous values less than -4 cm, while another 3% of the cells had depths greater than 100 cm which could be erroneous or real depths. As can be seen in figure 4.2, most of the depths that are either negative, or in the uncertain
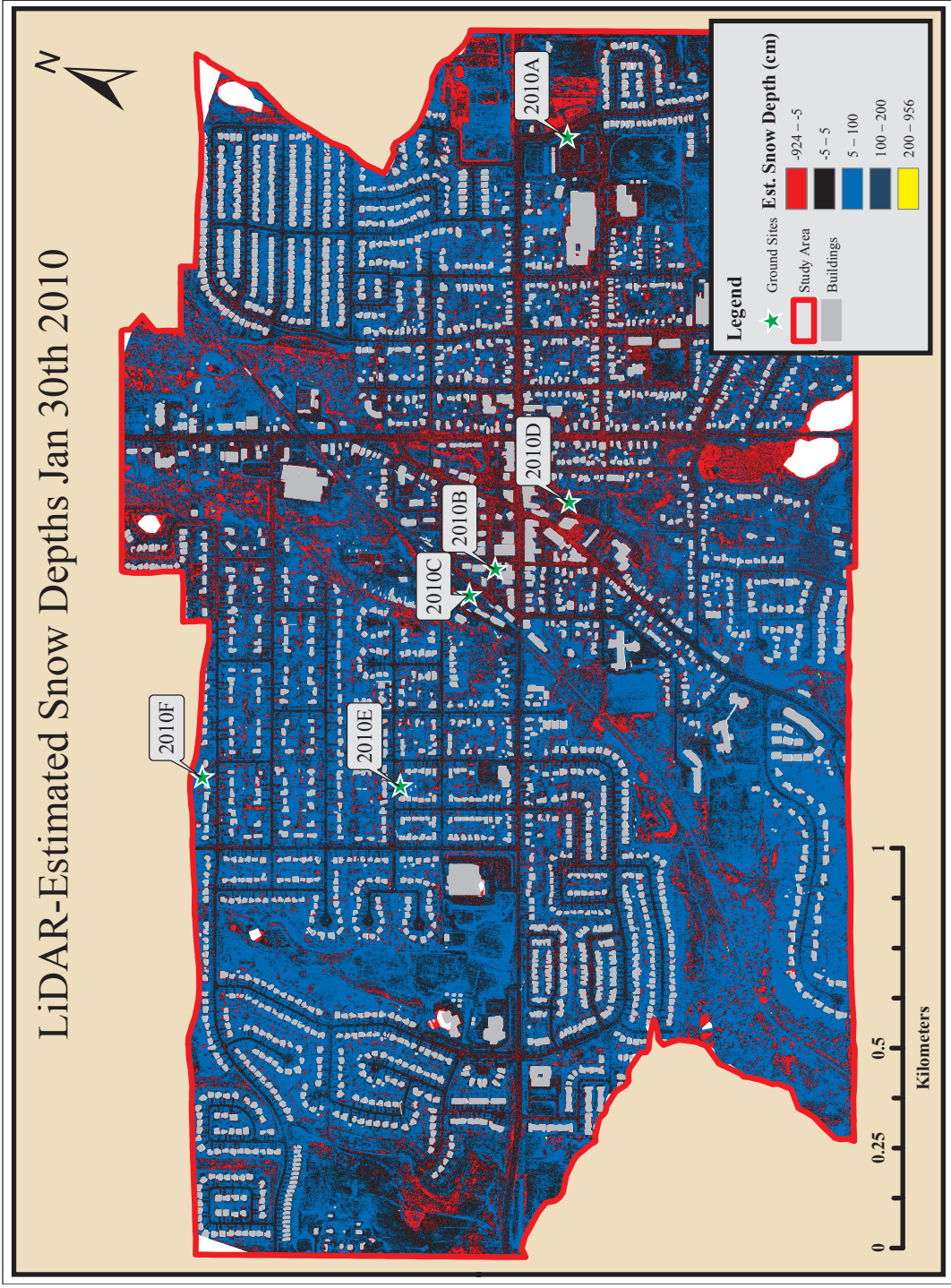
Figure 4.1: Map showing LiDAR-estimated snow depths as well as the locations of the ground collection sites for the January 30th, 2010 flight.
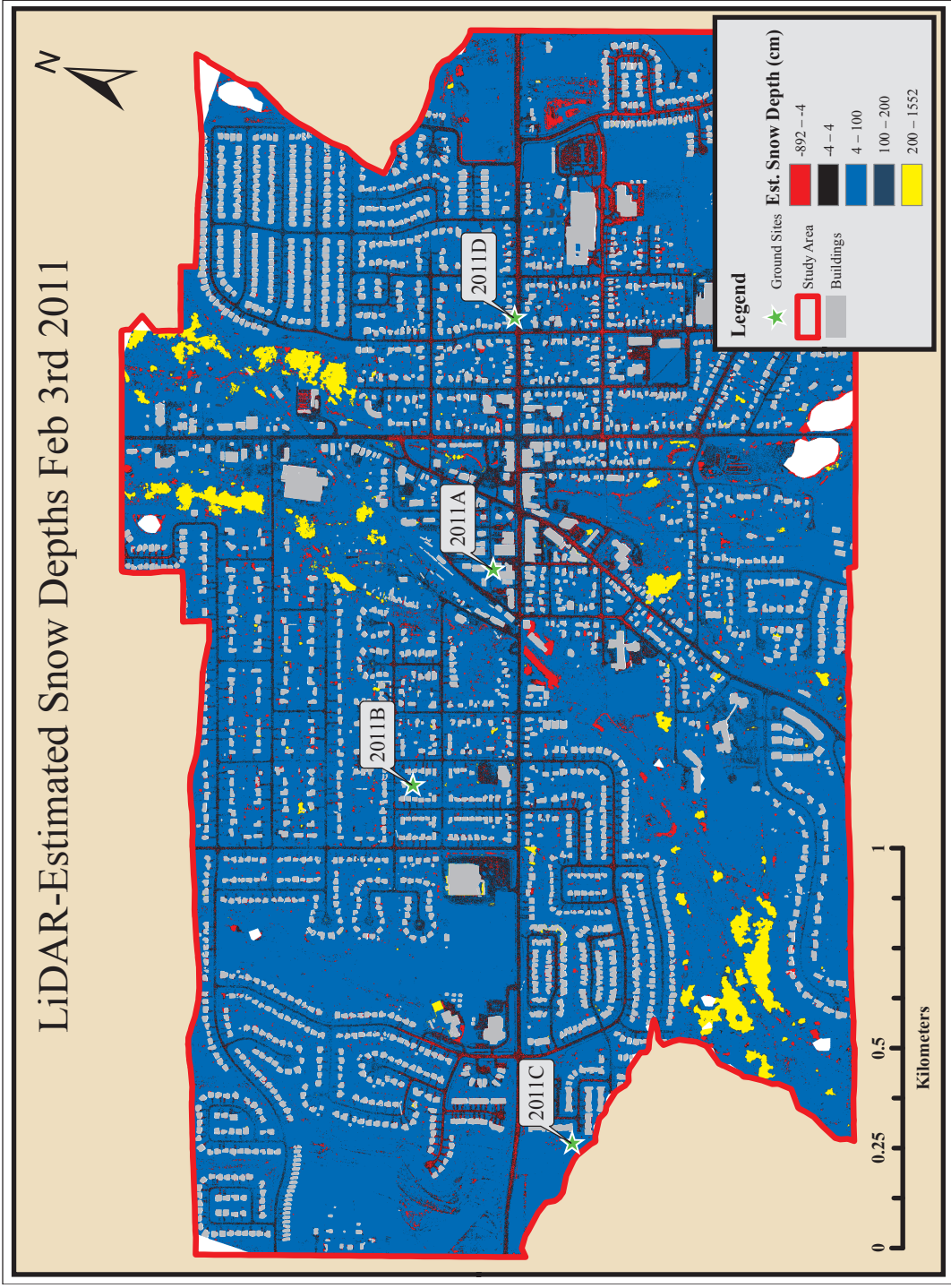
Figure 4.2: Map showing LiDAR-estimated snow depths as well as the locations of the ground collection sites for the February 3rd, 2011 flight.

Table 4.3: Number and percentage of cells contained in each of the 5 snow depth classes for the 2010 dataset shown in figure 4.1

Classification Range	Cell Count	Percentage
-924 cm – -5 cm	1895299	11.40%
-5 cm – 5 cm	5539919	33.32%
5 cm – 100 cm	9168613	55.15%
100 cm – 200 cm	18008	0.11%
200 cm – 956 cm	4505	0.03%

category are focused around the major roads which should have snow depths of zero. The areas where snow depths are greater than 200 cm are easily picked out in this map and are mostly located in densely forested areas. A closer look at these errors can be found in section 5.4, specifically in figure 5.3.

When comparing the two estimated snow depth maps, the 2010 map appears to have more variation between classes across the study area than the 2011 map. Notably, there are fewer cells in the categories below and close to zero and many more cells in the 4–100 cm category, in the 2011 dataset. The primary difference between the two snow depth maps is that there are many more estimates within the range of uncertainty in the 2010 dataset. Depths greater than 200 cm are also visible in the 2011 data while there are not enough to be seen in the 2010 dataset. The 2011 data appears to have less variability because the average snow pack was much deeper during the data collection period than it was in 2010. The difference in the average snow pack depth is described more in sections 4.3 and 4.4 below.

Table 4.4: Number and percentage of cells contained in each of the 5 snow depth classes for the 2011 dataset shown in figure 4.2

Classification Range	Cell Count	Percentage
-892 cm – -4 cm	651001	3.93%
-4 cm – 4 cm	1561662	9.42%
4 cm – 100 cm	13873487	83.69%
100 cm – 200 cm	156254	0.94%
200 cm – 1552 cm	335366	2.02%

4.3   Description of Ground Measured Snow Depths

Ground measurements were made at several sites during data collection period using the methods described in section 3.2.2. The measured snow depths for each site are summarized in figure 4.3 as well as tables 4.5 and 4.6. The average snow depth was much deeper during the 2011 winter season than during the 2010 winter season which is reflected in the mean measured snow depths of 12 cm in 2010 and 35 cm in 2011. Disturbed sites (marked with asterisks in tables 4.5 and 4.6) have consistently higher standard deviations for both years; they are also distinguishable based on higher maximum snow depths.

Figure 4.3 shows boxplot distributions of ground-measured (light grey) as well as LiDAR-estimated (dark grey) values for all sites in 2010 and 2011. The boxes represent the median (center line) 25th (lower) and 75th (upper) quartile ranges. The whiskers on the boxplot show the minimum and maximum values withing 1.5 times the inter-quartile range of the median. There is a much greater range of values in disturbed sites, especially during the 2011 winter season, because more measurements were taken in piled and banked snow. The 2010 disturbed sites have much less variation in the 25th to 75th percentile range because there were fewer measurements taken in disturbed snow in 2010. All of these measurements

are compared in figure 4.3 as well as in similar tables for the LiDAR-estimated snow depths in section 4.4 below.

Table 4.5: Descriptive statistics of ground measurements made on Jan. 31st, 2010

	All	2010A*	2010B*	2010C	2010D*	2010E	2010F
Mean (cm)	12	13	21	9	12	11	10
Min (cm)	0	1	0	4	2	4	1
Max (cm)	119	61	119	20	100	30	20
Std. dev. (cm)	14	13	27	4	22	5	4
Number	889	198	66	53	191	76	305

*Sites containing disturbed snow.

Table 4.6: Descriptive statistics of ground measurements made on Feb. 4th, 2011

	All	2011A*	2011B	2011C	2011D*
Mean (cm)	35	35	34	33	44
Min (cm)	0	0	13	6	0
Max (cm)	107	99	46	46	107
Std. dev. (cm)	16	23	5	6	25
Number	834	307	210	244	73

*Sites containing disturbed snow.

4.4   Description of LiDAR-Estimated Snow Depths

LiDAR measurements were extracted from the estimated snow depth maps to each point where ground measurements were taken using the methods in section 3.9. Figure 4.3 along with tables 4.7 and 4.8 show the distributions and descriptive statistics of each of the sites respectively. Similar to the ground-measured values, the LiDAR-estimated values in tables
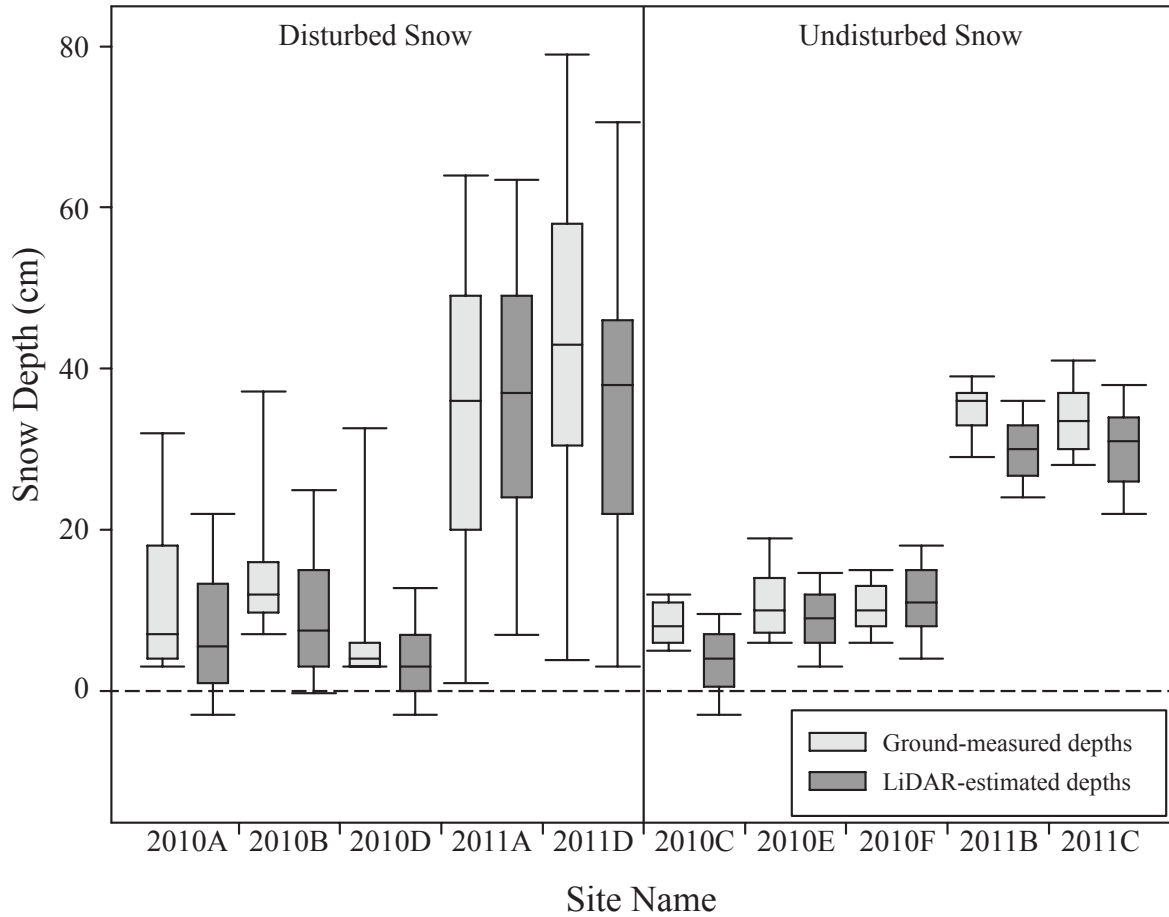
Figure 4.3: boxplot showing the distributions of ground-measured and LiDAR-estimated snow depths for each site. The sites to the left of the center line contain disturbed snow while the site to the right are undisturbed.

4.7 and 4.8 have higher standard deviations in disturbed sites. The disturbed sites also have much higher maximum values. The mean LiDAR-estimated snow depths were higher in 2011 (33 cm) than they were in 2010 (9 cm). The LiDAR-estimated minimum values are negative for some of the sites due to errors which are described in more detail in section

5.4. The minimum value for site 2011A is of specific interest because it shows a limitation of the ground filtering algorithm further described in section 5.4.2.

The boxplot distributions of the LiDAR estimates show that the 2011 snow depth estimates are deeper than the 2010 estimates. There is also much more variance in the 2011 LiDAR-estimated data, since more measurements were taken in disturbed snow in 2011. There is a much higher variation shown in the disturbed sites than there is in the undisturbed sites which is explained in detail in section 5.4.3.

Table 4.7: Statistics of LiDAR measurements at each ground measurement location collected on Jan 31st 2010

	All	2010A*	2010B*	2010C	2010D*	2010E	2010F
Mean (cm)	9	08	16	4	7	9	11
Min (cm)	-29	-07	-3	-12	-8	-2	-29
Max (cm)	131	45	131	11	85	27	24
Std. dev. (cm)	12	10	27	5	16	5	06
Number	889	198	66	53	191	76	305

*Sites containing disturbed snow.

Table 4.8: Statistics of LiDAR measurements at each ground measurement location collected on Feb 4th 2011

	All	2011A*	2011B	2011C	2011D*
Mean (cm)	33	37	30	30	36
Min (cm)	-53	-53	10	11	-4
Max (cm)	97	96	41	47	97
Std. dev. (cm)	16	22	5	7	23
Number	834	307	210	244	73

*Sites containing disturbed snow.

When comparing tables 4.5 and 4.6 with tables 4.7 and 4.8 respectively the mean of the LiDAR-estimated depths is lower than the ground-measured depths for all but sites 2010F and 2011A. The cause of these lower estimates is described in section 5.4.1. The standard deviations of ground-measured (tables 4.5 and 4.6) and LiDAR-estimated (tables 4.7 and 4.8) measurements are within 2 cm of each other for all sites except for site 2010D. The boxplot distributions of the LiDAR estimated depths shown in figure 4.3 have slightly larger interquartile range than the ground-measured depths.

4.5   Results of Accuracy Assessment

An accuracy assessment, described in section 3.9, was completed to compare each ground measurement to its associated pixels in the estimated snow depth maps for 2010 and 2011. The results of the accuracy assessment are presented in tables 4.9 and 4.10 as well as figures 4.4 and 4.5. Overall, both datasets have RMSEs that are less than the manufacturer-specified accuracy for the ALS but both datasets also show a negative bias in the LiDAR depth measurements. The accuracy assessment for each of the datasets are described for the two years below.

4.5.1   Accuracy Assessment of the 2010 Data

The accuracy assessment for the 2010 measurements show that on average the LiDAR-estimated snow depths have a RMSE of 11 cm when compared to the ground measurements. With a ground measured average of only 12 cm of snow for the 2010 LiDAR collection date, there is a large amount of uncertainty in the LiDAR measurements made during the 2010 season especially in the disturbed sites. The RMSE values in the disturbed sites are affected by the heterogeneity of the snow pack which is further described in section 5.4.3.

The undisturbed sites have smaller RMSE values and are within 2–3 cm of the RMSE of the overall dataset. The MAE and mean bias for most of the sites are negative meaning that the LiDAR underestimated snow depth in most cases, by an average of 3 cm. Site 2010A differs from the rest of the sites and has a positive bias which is described in more detail in section 5.4.1. The Spearman's rank correlation value for the entire 2010 dataset is 0.53, significant at the 99.9% confidence level, suggesting that the two datasets are moderately related to one another.
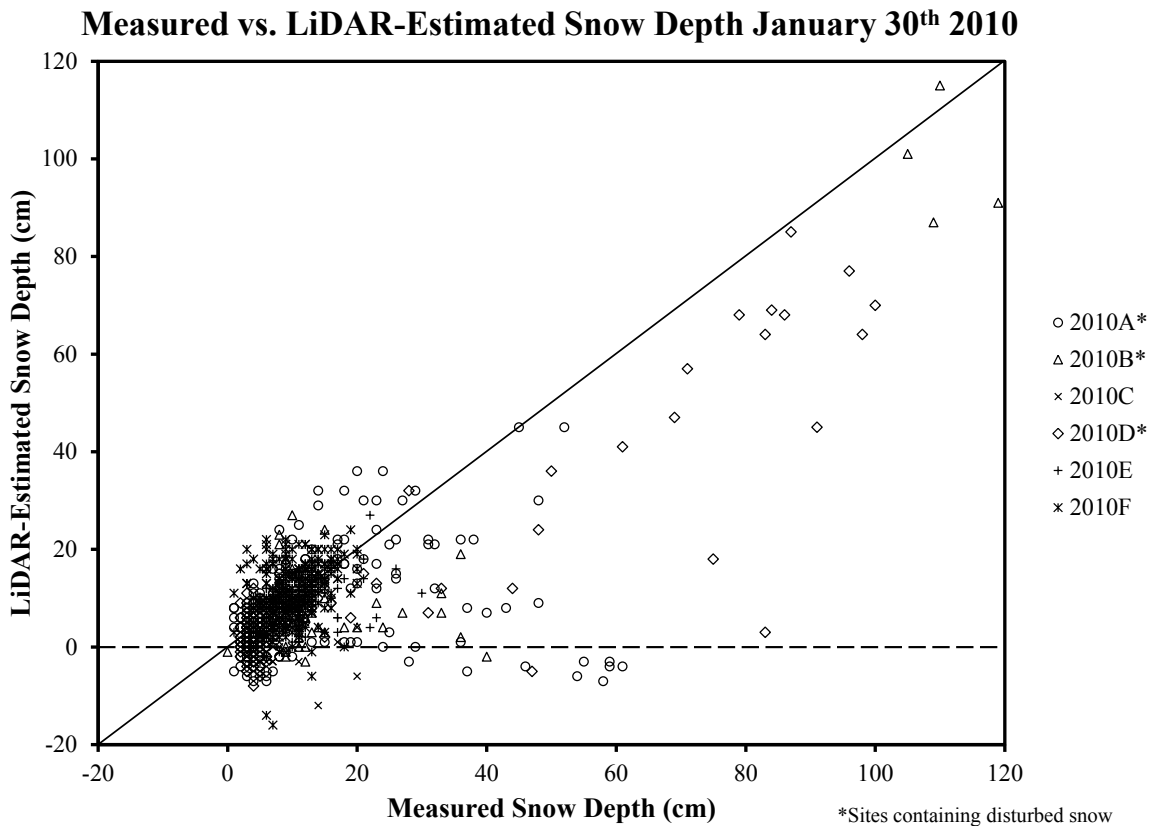

Figure 4.4: LiDAR-estimated snow depths compared with ground measured depths for all 2010 sites. The sites with disturbed snow are represented by closed symbols while the undisturbed sites are represented by open symbols.

Table 4.9: Comparative statistics between LiDAR and ground measurements for each 2010 site.

	All	2010A*	2010B*	2010C	2010D*	2010E	2010F
RMSE (cm)	11	15	12	8	11	6	6
MAE (cm)	3	5	5	5	5	2	0
Mean bias (cm)	-3	7	-5	-8	-5	-3	-1

*Sites containing disturbed snow.

Most of the 889 values can be seen clumped between 0 cm and 20 cm in both the ground and LiDAR measurements. The higher values collected in snow banks and piles are mostly below the identity line supporting the negative bias seen in most of the sites in table 4.9. There are also several LiDAR measurements below 0, the cause of which is described in more detail in section 5.4.

4.5.2   Accuracy Assessment of the 2011 Data

The measurements taken during the 2011 season had an average RMSE of 10 cm when comparing the LiDAR estimates to the ground measurements. Similar to the 2010 dataset the RMSE values were sightly higher in the disturbed sites due to more variation within the snow pack. The MAE and mean bias for all of the sites except 2011A are negative. Site 2011D has the largest bias with -8 cm, suggesting that snow depths were underestimated in all of the sites except for site 2011A. A Spearman's rank correlation coefficient of 0.72 for the 2011 dataset, significant at the 99.9% confidence level, shows that the LiDAR measurements are strongly related to the ground measurements made in the same locations. The relationship between the measurements can also be seen in figure 4.5.
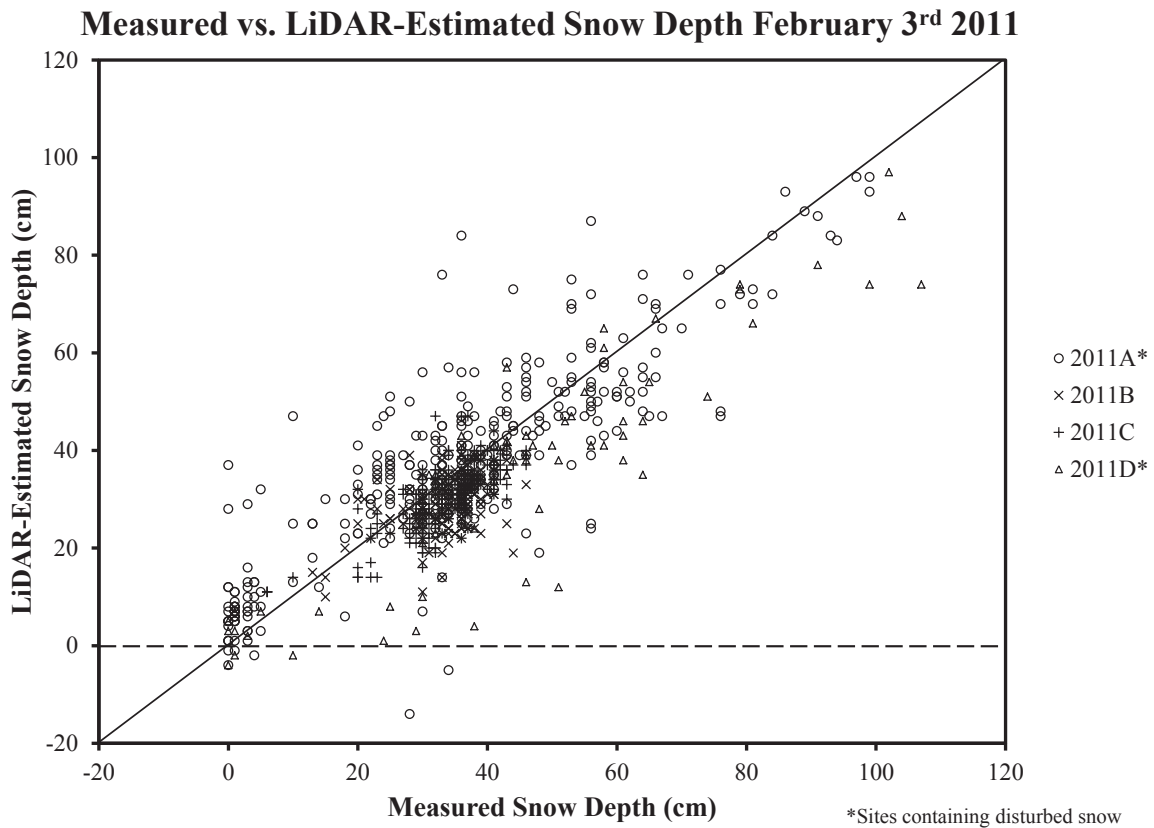
Figure 4.5: LiDAR-estimated snow depths compared with ground measured depths for all 2011 sites. The sites with disturbed snow are represented by closed symbols while the undisturbed sites are represented by open symbols.

LiDAR and ground measurements can be visually compared using figure 4.5. Most of the data points in the 2011 dataset are clumped in the 20–40 cm range. Negative bias is also shown in this figure since the majority of the points are noticeably below the identity line suggesting the LiDAR is underestimating snow depths. The small group of measurements close to 0 cm on the scatter plot are measurements that were made on cleared surfaces where snow depths were close to 0 cm.

Table 4.10: Comparative statistics between LiDAR and ground measurements for each 2011 site.

	All	2011A*	2011B	2011C	2011D*
RMSE (cm)	10	13	7	6	14
MAE (cm)	2	2	5	3	8
Mean Bias (cm)	-2	2	-5	-3	-8
*Sites containing disturbed snow.					

4.5.3 Accuracy Assessment of Complete Dataset

An accuracy assessment was completed on the entire dataset to determine the overall comparative statistics and correlations, as well as the differences between the disturbed and undisturbed sites. Table 4.11 contains the descriptive and comparative statistics for all disturbed and undisturbed sites collected in 2010 and 2011. The descriptive statistics shown in table 4.11 summarize the differences between LiDAR-estimated and ground-measured snow depths as well as undisturbed and disturbed sites. Overall, the LiDAR-estimated snow depths are lower for both the disturbed and undisturbed sites; this can be seen by looking at the mean values in table 4.11 as well as the biases. As seen in table 4.11 and explained in more detail in section 5.4.3, the RMSE of the disturbed sites is more than double that of the undisturbed sites.

Figure 4.6 is a scatter-plot showing all of the values from figures 4.4 and 4.5 along with an identity line for reference. Similar to what is seen in figures 4.4 and 4.5, the majority of the points in the scatter-plot appear to be below the identity line suggesting there is a bias in the data; this is also supported by the negative biases seen for both years in table 4.11. This shows that there is an overall underestimation of snow depth by the LiDAR in most of the data. Figure 4.6 shows more of a trend along the identity line than either of the

All Measured vs. LiDAR-Estimated Snow Depths
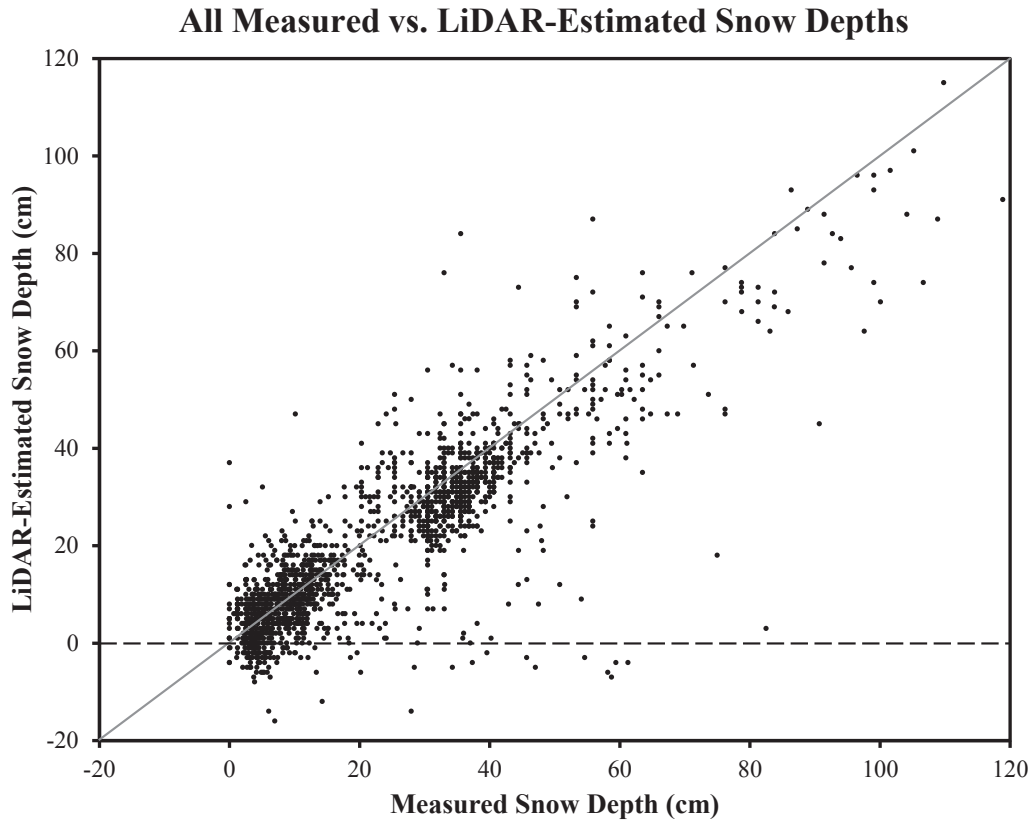
Figure 4.6: LiDAR-estimated snow depths compared with ground-measured depths for all 2010 and 2011 sites.

individual years because there is more variance in snow depths when compared to either of the individual datasets. Spearman's rank correlation coefficient was determined for the entire 2010 and 2011 dataset as well as for disturbed and undisturbed sites. The correlation coefficient was determined to be 0.83 for the entire 2010–2011 dataset, significant at the 99.9% confidence level. This suggests that the LiDAR measurements are very strongly correlated with the ground measurements over the whole dataset. When the disturbed and undisturbed sites were tested separately, Spearman's rank correlation coefficient was determined to be 0.764 and 0.860 respectively; both significant at the 99.9% confidence

Table 4.11: Descriptive and comparative statistics for all of the data for both years, as well as all of the data displayed by undisturbed and disturbed sites.

	All 2010 & 2011		Disturbed		Undisturbed	
	Ground	LiDAR	Ground	LiDAR	Ground	LiDAR
Mean (cm)	23	21	24	21	22	20
Min (cm)	0	-53	0	-53	1	-29
Max (cm)	119	131	119	131	46	47
Std.dev (cm)	19	19	24	24	13	12
Count	1723	1723	835	835	888	888
RMSE (cm)		10		13		6
MAE (cm)		3		3		2
Mean bias (cm)		-3		-3		-2

level. The LiDAR therefore appears to be more accurately estimating the depth of the snow pack in undisturbed sites as opposed to disturbed sites.

4.6 Summary of Results

Overall the RMSEs of both datasets are within the manufacturer-specified accuracy of the LiDAR system described in section 2.2. The RMSE of the disturbed sites is higher for both data collection periods due to the variance within the disturbed snow pack further described in section 5.4.3. The ALS underestimated the snow pack depth in the majority of the study sites throughout both data collection periods. This underestimation is shown by both the MAE and mean bias in tables 4.9, 4.10 and 4.11. Both of the datasets showed a strong correlation between the LiDAR and ground measurements significant at the 99.9% confidence level, but the 2010-2011 dataset shows a much stronger correlation. The strongest correlations (0.83) occurred when both datasets were combined because a greater range of snow depths was being compared.

The above tables and figures show that LiDAR is capable of estimating snow depths in both undisturbed and disturbed snow packs. A negative bias suggesting that the LiDAR is underestimating snow depths, as well as negative values present in the LiDAR measurements will be further discussed in chapter 5. The differences between the datasets from the two years and how these differences effect the end product will also be discussed in detail in the next chapter.

Chapter 5

Discussion

The results of this study indicate that ALSs are capable of estimating snow depth in both disturbed and undisturbed snow packs within a built-up environment. There is a statistically significant relationship between measured snow depths and LiDAR-estimated snow depths during both seasons of data collection used in this study. ALSs are capable of estimating snow depths to within 10 cm RMSE of ground-measured snow depths making it possible to characterize the distribution of snow within a built-up environment. This section will further explore the major findings of this study as well as the importance of these findings. Limitations and suggestions for further research related to this study will also be discussed.

5.1   Major Findings

The objective of this study was to present and evaluate a new method for measuring the distribution of snow in built-up environments using an ALS. A differencing method for estimating snow depth in built-up environments was presented in Chapter 3 with the

results and assessment being described in Chapter 4. The results presented from this study prove that ALSs are capable of estimating snow depths in built-up environments to within 10 cm average RMSE. These results are supported by a very strong correlation of 0.83 significant at the 99.9% confidence level using Spearman's rank correlation coefficient.

A further analysis of the results show that ALSs appear to provide more accurate estimates of snow depth in undisturbed snow than in disturbed snow with RMSEs of 6 cm and 13 cm respectively. The difference in the amount of error present in disturbed when compared to undisturbed sites is most likely caused by the amount of variance coupled with positional errors in the ground measurements described in section 5.4.3. This being said, the errors found in the LiDAR measurements for a disturbed snow pack are likely exaggerated in this report due to unavoidable positional errors in the ground-measured snow depths further described in section 5.4.3.

There is an average bias of -3 cm between the LiDAR-estimated and ground measured snow depth for the entire dataset as well as for most of the individual sites. This means that the LiDAR underestimated the depth of the snow by an average of 3 cm across the entire dataset. The most likely cause of this error is the difference between the ground reference between the LiDAR and depth probe. This bias is further described in sections 5.4.1 and 5.4.3. If this bias could be further quantified and removed based on land cover type, it would improve the overall performance of LiDAR at estimating snow depths.

The results from this study suggest that ALSs would be more appropriately used for estimating snow depths and distributions in regions with a deeper snow pack. The 2010 dataset had an average ground-measured depth of 12 cm with an overall RMSE of 11 cm meaning that 92% of the average depth could possibly be explained by error. The 2011

data on the other hand has an average ground-measured depth of 35 cm with an RMSE of 10 cm which means that only 29% of the average snow depth could possibly be explained by error. Errors in disturbed snow however are higher than errors in undisturbed snow and are most likely exaggerated due to positional errors made in the ground measurements. If these errors were minimized and the negative bias could be removed the overall performance of this method would improve for all snow depths. If an average RMSE of 6 cm could be achieved for the entire dataset the percentage of error for the two years would improve to 50% for 2010 and 17% for the 2011 dataset.

5.2   Importance of Major Findings

This study provides new methods for expanding the current body of knowledge on the distribution of snow in built-up environments. The validity of LiDAR-estimated snow depths has also been proven in this study over a range of land cover types as well as in disturbed and undisturbed snow packs. Although these methods have been used in several studies, little validation has been completed to date and no work has been completed within a built-up environment. The snow maps produced in this study could also be used to improve our understanding of urban hydrology in cold climates, particularly during snow melt. This section details the importance of the above findings and how they may be applied to future research.

As discussed in section 2.3.1, there has been very little research completed on the measurement of snow in built-up environments. The lack of knowledge in this area of research is primarily due to two issues: 1) the distribution of snow is difficult to measure in these environments (Matheussen and Thorolfsson, 2001), and 2) snow is often ignored in urban

hydrology under the assumption that rain events provide the highest amounts of runoff (Bengtsson and Westerstrom, 1992). Several studies have shown that in northern environments snow melt and especially rain on snow events can contribute to flooding in built-up environments more-so than heavy rainfall (Bengtsson and Westerstrom, 1992; Buttle and Xu, 1988; Ho and Valeo, 2005). A better understanding of how snow is distributed in an urban catchment would help urban hydrologists and hydrological engineers design new developments accordingly. The primary findings in this study outline a method that could be used to better understand how snow is distributed throughout built-up environments and therefore could help to design developments that are less prone to flooding during peak flow from snowmelt.

Having a more detailed view of how snow is distributed in built-up areas will be helpful for improving strategies for the re-distribution and removal of snow. Research has been occurring in recent years on how pollutants built-up in snow throughout the winter are being released in higher than average concentrations in some water courses (Engelhard et al., 2007; Viklander et al., 2003). Direct deposit of snow into waterways has been discontinued in many cities to prevent pollution from getting directly into waterways but there is still substantial uncertainty in the amount of these pollutants are being carried to waterways by runoff during snow melt(Viklander et al., 2003). A better understanding of how snow is distributed and re-distributed would assist in modeling where and how much polluted water is potentially contained within in urban catchments. Appropriate removal and disposal practices could then be designed to prevent overburdening urban catchments.

As mentioned previously in section 5.3 there have been several studies on the use of LiDAR for estimating the amount of snow on the ground but these studies are often based in extreme terrain or land cover conditions and are often not validated. Hopkinson et al.

(2004) validated LiDAR-estimated depths against ground measurements under different canopy types with limited success depending on canopy density, and type. Moreno Baños et al. (2011) attempted an assessment of the ALS data used in their study against 74 ground measured points in a mountainous environment. The results found in the study by Moreno Baños et al. (2011) were unsatisfactory due to positional errors in the GPS and other sampling errors forcing them to resort to other methods of validation. The validation presented in this study helps to add validation to previous studies completed which used LiDAR for estimating snow depth and should provide a source for validation of these measurements in the future.

5.3   Relation to Previous Studies

Several previous studies have used methods similar to the methods used in this study for determining how snow is distributed in different environments. Most of the previous work completed using these methods reference the work by Hopkinson et al. (2004) and Deems and Painter (2006) as validation for the LiDAR estimated snow depths used in their research. Although it is valid to assume similar accuracies given the same land cover type, equipment used, and methodology, validation should be performed if any of these factors are drastically changed. This study uses a very similar approach to work previously completed by Deems et al. (2006), Grünewald et al. (2010), Hopkinson et al. (2004), and Moreno Baños et al. (2011) but is focused on determining if these methods are applicable within a built-up environment. Built-up environments are very different from natural environments that have been studied previously. Differences such as man made objects (buildings, roads etc.) and anthropogenic re-distributed after snow has fallen add challenges to the methods used in previous studies. These challenges are addressed throughout this study and are

also addressed in section 5.4.

The results from this study cannot be compared directly to the results of the validation completed by Hopkinson et al. (2004) due to differences in methodology and outputs although some general similarities are apparent. The primary similarities found in the results between this study and the study completed by Hopkinson et al. (2004) were that there is an underestimation of the snow depth due to vegetation in some areas, and that snow accumulation within the canopy of coniferous trees can cause an overestimation of snow depths. Hopkinson et al. (2004) found that snow depths in deciduous forests were being underestimated due to errors in the snow free DEM caused by a dense forest understory. A similar underestimation was found in this study that is most likely caused by a combination of vegetation on the ground and the difference between the ground reference as recorded by the LiDAR and the snow depth probe. Overestimation of snow depths in coniferous forests were found in the 2011 snow depth map but were not present in the 2010 map for this study. Hopkinson et al. (2004) noted similar overestimation in their study site which were thought to be caused by snow accumulation within the canopy in the winter dataset. Since these errors were present in the 2011 data, when there was a much larger average snow depth, it has been assumed that the errors found in this study are due to similar circumstances. There was also a similarly strong association between measurements in this study and the measurements in the study completed by Hopkinson et al. (2004) suggesting that similar results can be attained in forested and built-up environments.

Moreno Baños et al. (2011) calculated RMSE for their LiDAR-estimated snow depths similar to this study but segregated their dataset by slope angle. Whilst the RMSE values from this study cannot be directly compared to the RMSE values from the study by Moreno Baños et al. (2011), some assumptions can be made based on RMSEs calculated during this

study. Moreno Baños et al. (2011) were unable to compare ground measurements directly to their LiDAR estimated values because of positional GPS errors and the variability of the terrain in their study site. To validate their measurements Moreno Baños et al. (2011) used air photos to digitize areas where there was no snow present (0 cm) and computed an RMSE against LiDAR-estimated values within the no-snow areas. This method allowed them to compare 680000 LiDAR measurements against a snow depth of 0 cm with an overall RMSE of 43 cm in areas where slope was $< 60°$. The validation methods used by Moreno Baños et al. (2011) could be compared to the relative accuracy assessment completed in this study which was used to determine the accuracy of the three DEMs. The relative accuracy assessment for this study (section 4.1) produced RMSEs of 5 cm and 4 cm for 2010 and 2011, respectively. The transects used for the relative accuracy assessment in this study did not contain slopes $> 20°$. Moreno Baños et al. (2011) calculated the RMSE of slopes $< 20°$ (18.5% of the total dataset) in their study to be between 17 cm and 18 cm. The RMSE of their estimated snow depths would therefore be at minimum 17–18 cm. Snow depths estimated in this study were all found to have RMSE ≤ 15 cm proving that ALSs are comparable at estimating snow depths in a built-up and mountainous environments.

The results from the two previously validated studies were compared with the results from this study to show that LiDAR appears to estimate snow depths equally well in natural and built-up environments. Although other studies such as Deems et al. (2006) were able to validate their data using the study by Hopkinson et al. (2004), differences in the land cover made it necessary for the data to be validated within a built-up environment before these data could be used for further analysis.

5.4 Study Limitations and Causes of Error

With the exception of sites 2010A and 2011A, snow depth estimates made using the ALS in this study underestimated snow pack depth. Negative snow depths were also recorded in both datasets, occurring mostly on areas where a depth of 0 cm was expected. Possible causes of underestimated and negative snow depths are 1) unknown biases in the ALS data not quantified during the relative accuracy assessment, 2) errors in one of the DEMs caused during the ground classification process, and 3) differences in the ground reference between the ALS and depth probe. Snow depths that were above the expected value also occurred in both datasets but are more prominent in the 2011 dataset. Erroneous positive snow depths are mostly caused by errors in one or more of the DEMs created during the ground classification process. All of the above errors as well as the positive biases seen in sites 2010A and 2011A are further discussed below.

5.4.1 Causes of Biases in the ALS Data

As previously mentioned there is a negative bias seen in most of the study sites causing the ALS to underestimate snow depth when compared to the ground based measurements. The most likely cause of this underestimation is a difference in what the ALS and depth probe measure as the ground reference (further described in section 5.4.3). This negative bias could also be caused by unexplained biases in the ALS data not quantified during the relative accuracy assessment. If this is the case, the percentage of negative snow depths found on roads and other flat surfaces would also be explained. Biases in the ALS data can be caused by a variety of conditions during the collection and processing steps including GPS error, calibration accuracy, and errors in the processing methods (Ussyshkin et al., 2008). Calibration of each of the ALSs used for this study was verified to be within

68

manufacturer specifications for each flight by Optech Inc. As described in section 2.2 the manufacturer-specified absolute accuracy of Optech's ALTM at the settings used for this study is ±15 cm with attainable absolute accuracies as low as ±12–13 cm (Ussyshkin and Smith, 2006). This study tested the relative accuracy of the datasets with RMSEs of 5 cm and 4 cm for the 2010 and 2011 data respectively. The scale at which the relative accuracy assessment was completed could have caused smaller scale, positive and negative biases to cancel each other out. A further accuracy assessment at the scale of each of the study sites would confirm the accuracy of each of the accumulation datasets relative to the bare earth dataset on a site by site basis.

Sites 2010A and 2011A are different from the rest of the sites because the LiDAR-estimated snow depths show a positive bias over the ground-measured depths. The only similarity between the two sites is that they both contain disturbed snow. The cause of the positive bias in these sites was further investigated to explain why these two sites differ from the rest of the sites and to add validity to the negative biases seen in the other sites. It was noted upon further investigation that both of these sites contain transects located on areas with very little snow directly beside a snowbank. The snow depth probe would therefore be reporting depths close to 0 cm while the 50 cm pixels in the ALS data represent an average which could include parts of the snowbank. Figure 5.1 shows a snow depth transect from site 2011A along with the LiDAR-estimated values from that transect. The LiDAR-estimated depths in figure 5.1 have an average of 6 cm while the ground-measured depths have an average of only 2 cm. This overestimation could also be exaggerated by positional errors in the ground measurements further described in section 5.4.3.
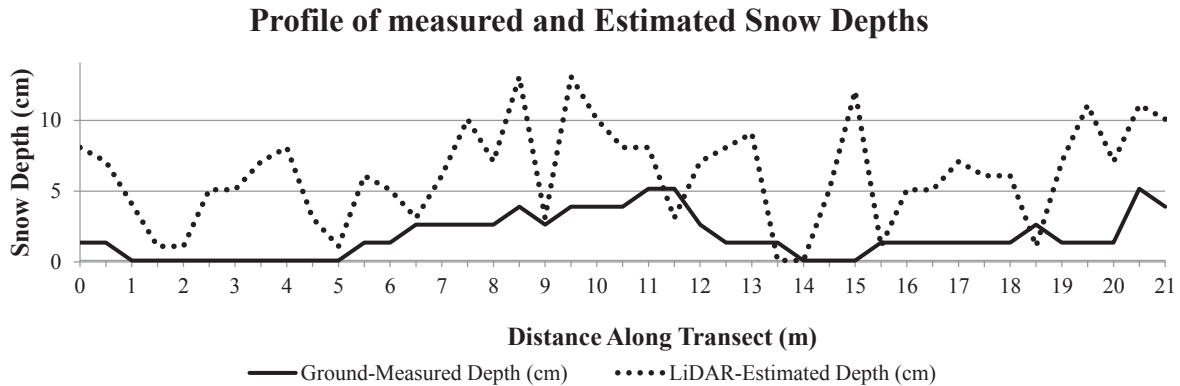
Figure 5.1: This graph shows the overestimation of snow depths by the LiDAR for a transect beside a snowbank.

5.4.2 Causes of Errors Within the DEMs

Errors in either of the DEMs can cause overestimation or underestimation of snow depth in the final snow depth map. These errors are mostly caused during the ground classification process described in section 3.4 which is explained in more detail by (Axelsson, 2000). The ground classification algorithm used in this study, as with all LiDAR ground classification algorithms, has limitations in its ability to classify ground points, especially in very dense forest, around buildings of different sizes, and in areas with complex mixed land cover Meng et al. (2010). The datasets classified for this study are no exception to these limitations. Each of the three datasets has certain areas where the ground was not classified properly, which are mostly around buildings, and dense forest areas. 5.3 shows three sites containing either positive or negative snow depth errors and their related DEMs.

Site 1 in figure 5.3 (A–D) is a densely forested area where snow depths were unreasonably high (200–800 cm). High depth estimates are much more prominent in the 2011 data than they are in the 2010 data, which can be seen when comparing tables 4.3 and 4.4 from

the results section. Upon closer inspection it was noticed that the bare earth DEM as well as the 2010 snow accumulation DEM had very similar elevations. The 2011 snow accumulation DEM however, contained much higher elevations which can be seen in figure 5.3c. The reason the 2011 DEM contains much higher elevations at site 1 in figure 5.3 is most likely due to snow accumulation within the forest canopy of the coniferous trees present in this location. Snow accumulation within the tree canopy would prevent LiDAR pulses from reaching the ground causing the ground filtering algorithm to classify canopy as ground. These errors would only be present in the 2011 data because there was much more snow present in 2011 than there was in 2010. Hopkinson et al. (2004) noted similar overestimates, occurring in low lying conifer vegetation in their 2004 study.

In figure 5.3, figures E–H show a section of site 2011A where there is a loading dock present behind a building. Manual snow depths were collected on and around the loading dock which are represented by yellow circles in figure 5.3 E–H. Unfortunately the ground classification algorithm classified the loading dock as ground in the bare earth DEM (figure 5.3f), while it was not classified as ground in the 2011 snow accumulation DEM (figure 5.3g). The absence of the loading dock in the 2011 DEM caused negative snow depths to be estimated which can be seen in red in figure 5.3H. The ground classification algorithm classified the loading dock as ground in the 2009 data because there were many ALS points on the dock which with the building removed were within the angle threshold to be classified as ground points. The 2011 ALS data had very few points on the loading dock and these points were most likely removed as isolated points. Errors such as these are hard to quantify but make up a very small amount of the dataset making up a negligible percentage of the entire dataset.
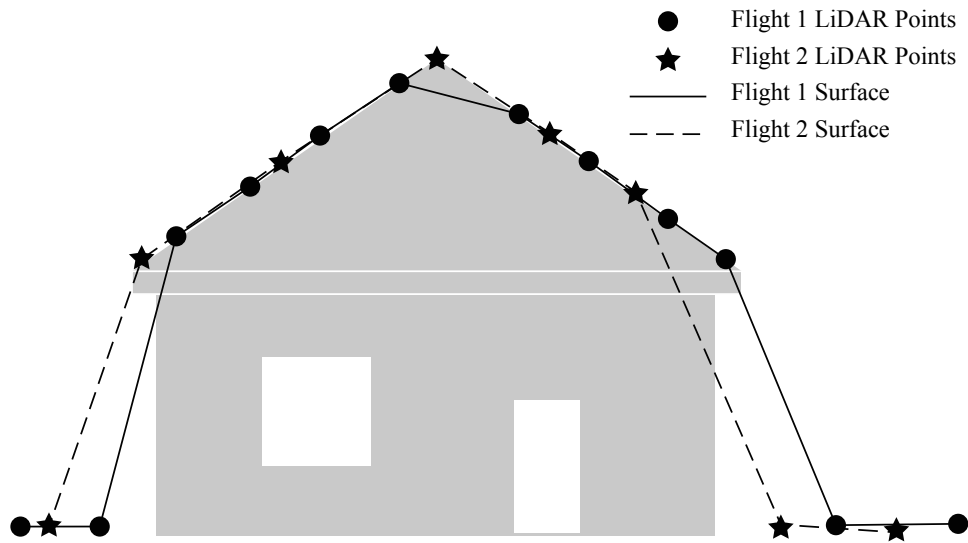
Figure 5.2: This image shows points and interpolated surfaces from two flights over a building. Large errors on either side of the building as well as on the peak would be present if the surfaces were differenced.

Site 3 in figure 5.3 contains two types of error that are visible in the estimated snow depth maps. The first is visible in yellow or red around the edges of the buildings seen in figure 5.3L. These errors are present when the ground classification algorithm included a building in one of the DEMs, and the building mask did not fully mask the edges of a that building. Positive or negative snow depths, equivalent to the height of a building, will be present on the snow depth map if a building is not fully removed from one or more of the DEMs. Figure 5.2 shows LiDAR points from 2 flights as well as the possible interpolated surfaces from these points. If the two surfaces were differenced, large errors in snow depth would occur at both sides and along the peak of the roof. If the building mask was not applied to the DEMs before they were differenced, more of these errors would have occured. The second type of errors seen in figure 5.3L are present on areas that should have a snow
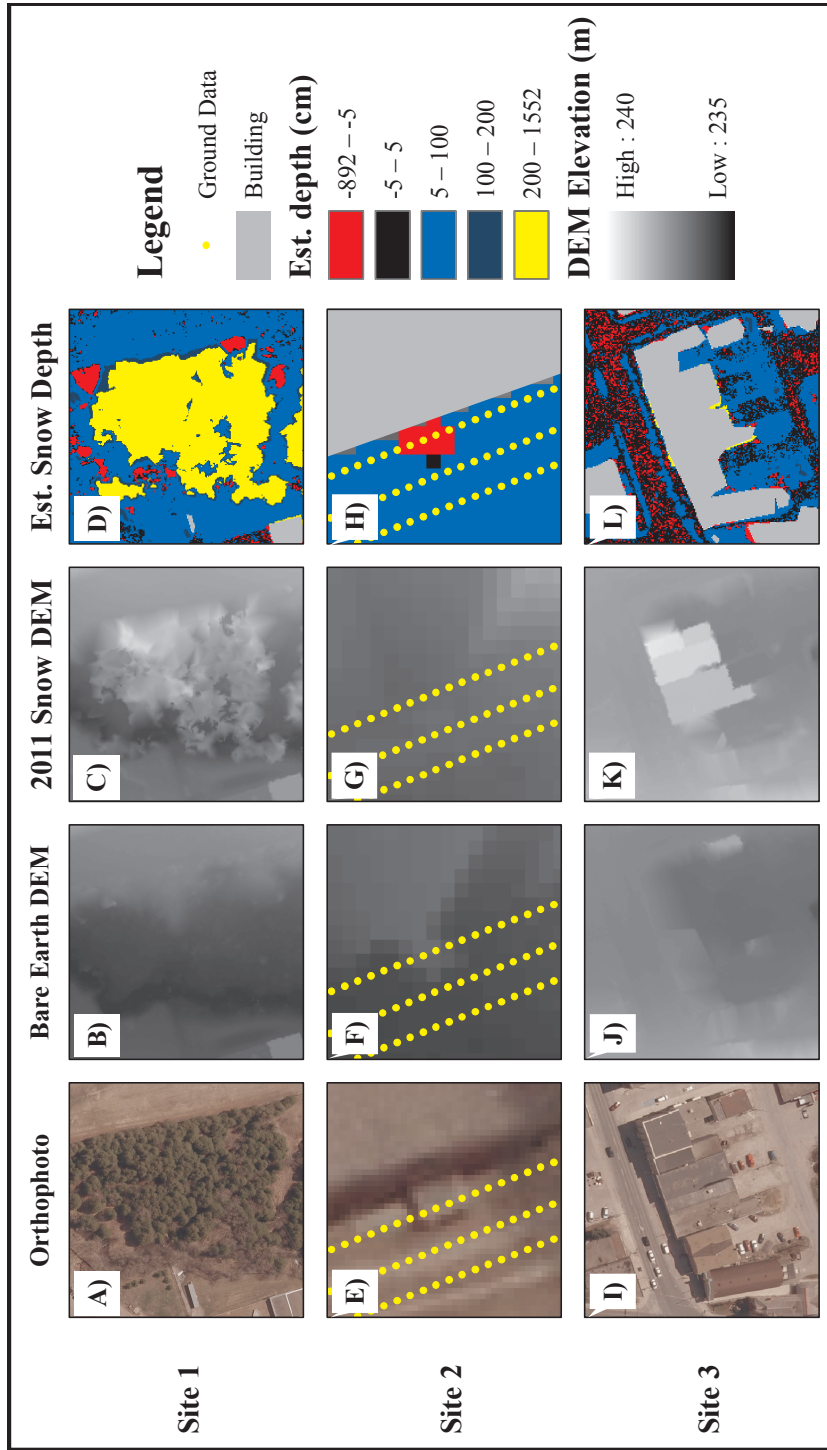
Figure 5.3: This figure shows orthophoto, DEMs, and snow depth classifications for 3 sites which contain erroneous snow depth values. Site 1 contains overestimated values due to dense tree canopy covered with snow. Site 2 contains underestimated values because of a loading dock that was not removed from one of the DEMs. Site 3 contains overestimated values around the edge of a building as well as underestimated values along a road (J D Barnes Limited, 2008).

depth of 0 cm such as cleared roads and parking lots. These are mostly negative errors between -4 cm and -10 cm and are much more prominent in the 2010 data than they are in the 2011 data. The 2011 data is similar to the study completed by Hopkinson et al. (2004) where negative snow depths made up a negligible percentage of the total error. The 2010 data however, contains nearly 3 times as many erroneous values with 11.40% of the snow depth map containing negative values below -5 cm. The reason that there are so many more errors in the 2010 data is that there wasn't enough snow in several areas to register positive snow depths.

Another cause of error that is present in both of the snow depth maps are physical changes in the surface between two ALS flights such as changing water levels, industrial stock piles, or construction. Changes in water level can be seen causing negative values directly to the southwest of site 2010D in figure 4.1. There is a pond that would have had a higher water level in the fall than the ice formed through the winter causing negative snow depths to occur. As mentioned above, stock piles in industrial areas that change in volume as well as construction sites where fill is moved around to reshape the terrain will cause errors in the estimated snow depth. Although these errors are hard to avoid, they cause a negligible amount of error.

5.4.3 Causes of Error in the Snow Depth Measurements

The two different methods of measuring snow depths used during this study are described in section 3.2.2. Both the automated and manual methods of collecting snow depths have sources of error that could effect the overall accuracy of this study. Both methods are subject to error due to differences between what the ALS and depth probe record as the ground reference, as well as positioning errors.

Differences between what is considered the ground for the ALS and ground based measurements could explain the negative bias seen in most of the site comparisons. An ALS receives a returning waveform for each pulse of light sent out and digitizes a discreet point on that waveform that represents the distance to the object the pulse reflected off of (further described in section 2.1) (Höfle and Pfeifer, 2007). The footprint of an ALS pulse at the settings used for this project is approximately 25 cm on the ground. The waveform that is recorded by the system represents the amount of laser light reflected off of everything in that 25 cm footprint (Baltsavias, 1999). If there is low vegetation in the footprint such as grass the ALS pulse may not be able to penetrate all the way through the vegetation and could digitize a point that is a few centimeters above the actual ground; This is shown on the right side of figure 5.4 as well as in work completed by Hopkinson et al. (2005) and Hodgson and Bresnahan (2004). The snow depth probe is capable of penetrating through all of the snow and low lying vegetation until it hits frozen ground as seen on the left side of figure 5.4. The frozen ground could be several centimeters below what the ALS has measured as a ground return. This difference would cause the LiDAR-estimated snow depth to be less than the ground-measured snow depth causing a bias. This is most likely the primary explanation for the negative bias seen in the LiDAR on all sites except for 2010A and 2011A.

Both of the ground datasets contain a certain amount of positioning error from GPS receivers used to collect the positions. The automated snow depth probe used to collect the 2010 ground data uses a Garmin GPS16 which uses the wide area augmentation system to provide an accuracy of <3 m. The antenna for the GPS is attached to the backpack which holds the data logger for the automated snow depth probe. This adds another 0.2–1 m of positional uncertainty because the actual snow depth measurement is made
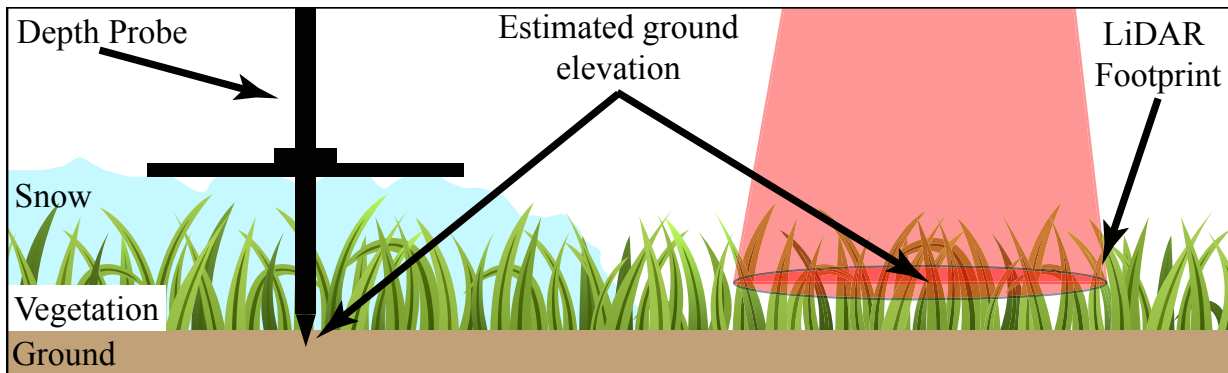
Figure 5.4: This figure shows the difference between the ground as measured by a depth probe and as measured by the LiDAR. The LiDAR may not be able to penetrate to solid ground while the depth probe penetrates the snow pack until it hits frozen ground.

by the snow depth probe which is held by the user. The probe is therefore an unknown distance in an unknown direction from the antenna when each measurement is taken. This means that each measurement taken using the automated snow depth probe has a positional uncertainty of <4 m. For the manual snow depth measurements described in section 3.2.2.2 the average of more than 50 GPS positions was taken and differentially corrected at both ends of each transect this provided an accuracy of <1 m for the ends of each transect. Measurements were then made at a 0.5 m interval measured using a tape measure between the two points. The positional accuracy of the manually collected snow depth should therefore be <1 m which is an improvement over the automated collection method.

The positional uncertainties described above add uncertainty to the accuracy assessment described in sections 3.9 and 4.5. This uncertainty is present because each ground measurement is not necessarily located within the exact pixel on the snow depth map where that measurement was taken. Even if the ground measurement is located within the appropriate

pixel in the LiDAR data the ground measurement is a point within that 0.5 m by 0.5 m pixel which does not necessarily represent the average snow depth within that pixel. These uncertainties have more impact in disturbed snow where there is much more variance in snow depth as seen in sections 4.3 and 4.4. The accuracies reported for disturbed snow in this study are likely lower than reality due to the positional uncertainties described above.

5.5   Summary of Discussion

The major outcome of this research is that ALSs are capable of estimating snow depth in a built-up environment to within 10 cm RMSE. Better estimates of snow depth occur in areas that receive a deeper snow pack and areas where snow is undisturbed. There is an overall underestimation of the depth of snow as measured by the ALS which is most likely due to differences in what the ALS and depth probe measure as the ground. If this bias was removed, the overall accuracy of the LiDAR estimated snow depths would improve. Other errors are introduced into the DEMs around buildings and dense forest but these have been minimized through masking of the buildings and only make up a small percentage of the estimated depths.

Chapter 6

Conclusions

The objective of this thesis was to present and evaluate a new method for measuring the distribution of snow depths within built-up environments, by differencing elevations collected by an airborne laser scanner before, and during peak snow accumulation. The results from this study have shown that:

1. The methods presented in this study are capable of estimating snow pack depth to within 10 cm average RMSE, providing the capability to create high spatial resolution maps of snow distributions in built-up environments.

2. A statistically significant relationship was found between LiDAR-estimated and ground-measured snow depths with higher correlation in sites containing undisturbed snow when compared to sites containing disturbed snow.

3. An average bias of -3 cm was found between the LiDAR-estimated and ground-measured snow depths which represents and underestimation of snow depth by the ALS. This underestimation is most likely due to differences in the respective ground elevation references in the ALS and depth probe measurement processes.

To summarize, this thesis has shown that it is possible to estimate snow depths in built-up environments using ALS technologies. A small negative average bias is present in most sites throughout both years of data, due to differences in how the ALS and depth probe determine the ground reference. The overall accuracy of the methods presented in this thesis would improve if the mean bias could be systematically removed based on land cover type. Although several other sources of possible error are examined throughout this thesis, the majority of the LiDAR-estimated snow depths are within the expected range. The methods described through this thesis would be best suited for regions that experience high amounts of accumulation to minimize the relative error present in the depth estimates. These methods also make it possible to map the distribution of snow in built-up areas, which is otherwise a difficult and time consuming task. High resolution snow depth maps will help to characterize how snow is distributed and re-distributed in built-up environments. By quantifying the distribution of snow within urban catchments, it is expected that this technology will be able to improve infrastructure design, thereby facilitating the improvement of snow removal practices and preventing flooding during spring melt periods.

6.1   Future Research

Future research related to this thesis should be focused in two main areas. The first is the improvement of the methods and our understanding of the errors that occur; secondly, the methods used in this study need to be applied in urban winter hydrology to improve the understanding of how snow is distributed in built-up environments. Methods used in the validation for this thesis could also be applied to other land cover types to provide a better understanding of the accuracy of ALSs for estimating snow depth across multiple

land cover types.

To improve the methods and minimize errors in this study there are several topics that should be explored in the future. These topics include: minimizing positional errors in ground measurements, quantifying the negative bias seen in the LiDAR-estimated depths, and exploring the possibility of measuring snow on roofs. One of the main causes of error, especially in the 2010 data was the positional uncertainty in the ground measurements. The positional error in the 2011 dataset (<1 m) was an improvement over the 2010 data (<4 m) but more improvement could be made with the use of survey grade, sub-decimeter accuracy GPS equipment. Using sub-decimeter level GPS receivers would improve the likelihood of a snow depth measurement being contained in the appropriate pixel in the finished snow depth map which would minimize errors such as the ones described in section 5.4.3.

As described in section 5.4.1 there is an overall negative bias seen in most of the study sites in this study. It has been suggested that this bias is most likely caused by differences in ground reference between the ALS and snow depth probe. Both Hopkinson et al. (2005) and Hodgson and Bresnahan (2004) showed that low lying vegetation will cause an overestimation in the elevation of the ground because most of the LiDAR pulse will reflect off of vegetation and not the ground. To improve the accuracy of this study, a high resolution map of different types of land cover such as low grass, high grass and pavement with defined average bias values could be used to correct for biases. Minimizing or removing biases would improve the overall accuracy of the snow depth estimates, improving the overall quality of the final snow depth maps.

For this study buildings were completely removed from the DEMs to reduce the amount of errors caused around the edges of buildings which are described in section 5.4.2 and figure 5.2. Further research should look at masking only the edges of buildings to include building roofs in the estimated snow depth maps. To include snow depths on building roofs in this study a much higher resolution dataset would need to be collected in both the fall and winter to minimize errors around the edges and at roof peaks. Some of the snow on building roofs will eventually melt and end up on the ground as an input of water to the catchment, and should therefore be quantified. This data could also be used to map snow loading on building roofs to monitor possible dangers from overloading in regions with heavy snowfall.

The objective of this study was to present and evaluate a new method for measuring the distribution of snow depths within built-up environments. To expand on this research the next step is to characterize the distribution of snow within built-up environments and apply this knowledge to urban hydrological studies. As pointed out by Matheussen and Thorolfsson (2001) it is difficult to measure the distribution of snow in built-up environments; however, these measurements are needed to better model urban runoff for sustainable infrastructure design (Ho and Valeo, 2005). The methods presented in this study make it is possible to determine the distribution of snow depths within a built-up environment. Distributions, coupled with the water equivalent of different types of snow such as those defined by Ho and Valeo (2005) would allow better forecasting of runoff in urban catchments. Once this has been completed the estimated snow water equivalent volumes could be compared to measured runoff values to determine the possibility of predicting runoff from these measurements.

References

Aoki, T., Aoki, T., Fukabori, M., Hachikubo, A., Tachibana, Y., and Nishio, F. (2000). Effects of snow physical parameters on spectral albedo and bidirectional reflectance of snow surface. *J. Geophys. Res.*, 105(D8):10219–10236. 19

Axelsson, P. (2000). DEM generation from laser scanner data using adaptive TIN models. *International Archives of Photogrammetry and Remote Sensing.*, XXXIII:110–117. 7, 36, 37, 70

Baltsavias, E. (1999). Airborne laser scanning: Basic relations and formulas. *ISPRS Journal of Photogrammetry & Remote Sensing*, 54:199–214. 6, 7, 9, 10, 75

Beaglehole, D., Ramanathan, B., and Rumberg, J. (1998). The UV to IR transmittance of Antarctic snow. *J. Geophys. Res.*, 103(D8):8849–8857. 21

Bengtsson, L. and Westerstrom, G. (1992). Urban snowmelt and runoff In Northern Sweden. *Hydrological Sciences Journal-journal Des Sciences Hydrologiques*, 37(3):263–275. 64

Boyd, D., W.R., S., and Taylor, D. (1981). Snow and buildings. In Gray, D. M. and Male, D. H., editors, *Handbook of Snow: Principles, Processes, Management & Use*, chapter Part III: Snow and Engineering, pages 3–13. Pergamon Press Canada, Toronto. 2, 16

Buttle, J. M. and Xu, F. (1988). Snowmelt runoff in suburban environments. *Nordic Hydrology*, 19(1):19–40. 16, 64

Chang, A. T. C., Kelly, R. E. J., Foster, J. L., and Hall, D. K. (2003). Global SWE monitoring using AMSR-E data. 18

City of Toronto (2011). City of Toronto 2011 budget. http://www.toronto.ca/budget2011/ Accessed July 10th 2011 [Electronic]. 2

Davis, R. E., Painter, T. H., Cline, D., Armstrong, R., Haran, T., McDonald, K., Forster, R., and Elder, K. (2008). NASA Cold Land Processes Experiment (CLPX 2002/03): Spaceborne Remote Sensing. *Journal of Hydrometeorology*, 9(6):1427–1433. 18

Deems, J. S., Fassnacht, S. R., and Elder, K. J. (2006). Fractal distribution of snow depth from LiDAR data. *Journal of Hydrometeorology*, 7(2):285–297. 1, 17, 18, 21, 23, 24, 65, 67

Deems, J. S. and Painter, T. H. (2006). LiDAR measurement of snow depth: Accuracy and error sources. In *Proceedings of the International Snow Science Workshop ISSW. Telluride, CO, USA, 16 October 2006*, pages 384–391. 1, 2, 6, 8, 10, 12, 17, 21, 24, 65

Dozier, J., Green, R. O., Nolin, A. W., and Painter, T. H. (2009). Interpretation of snow properties from imaging spectrometry. *Remote Sensing of Environment*, 113:S25–S37. 20

Egli, L., Jonas, T., Grnewald, T., Schirmer, M., and Burlando, P. (2011). Dynamics of snow ablation in a small alpine catchment observed by repeated terrestrial laser scans. *Hydrological Processes*. [Accepted Article]. 1, 22

Elder, K., Cline, D., Goodbody, A., Houser, P., Liston, G. E., Mahrt, L., and Rutter, N. (2009a). NASA Cold Land Processes Experiment (CLPX 2002/03): Ground-Based and Near-Surface Meteorological Observations. *Journal of Hydrometeorology*, 10(1):330–337. 2

Elder, K., Cline, D., Liston, G. E., and Armstrong, R. (2009b). NASA Cold Land Processes Experiment (CLPX 2002/03): Field Measurements of Snowpack Properties and Soil Moisture. *Journal of Hydrometeorology*, 10(1):320–329. 13

Elder, K., Dozier, J., and Michaelsen, J. (1991). Snow accumulation and distribution in an alpine watershed. *Water Resources Research*, 27(7):1541–1552. 13, 17

Engelhard, C., De Toffol, S., Lek, I., Rauch, W., and Dallinger, R. (2007). Environmental impacts of urban snow management - The alpine case study of Innsbruck. *Science of the Total Environment*, 382(2-3):286–294. 64

Environment Canada (2011). Canadian climate normals or averages 1971-2000. Accessed June 19th 2011 (electronic). 26

Grünewald, T., Schirmer, M., Mott, R., and Lehning, M. (2010). Spatial and temporal variability of snow depth and ablation rates in a small mountain catchment. *The Cryosphere*, 4(2):215–225. 21, 22, 65

83

Ho, C. L. I. and Valeo, C. (2005). Observations of urban snow properties in Calgary, Canada. *Hydrological Processes*, 19(2):459–473. 2, 13, 16, 17, 19, 64, 81

Hodgson, M. E. and Bresnahan, P. (2004). Accuracy of airborne lidar-derived elevation: Empirical assessment and error budget. *Photogrammetric Engineering & Remote Sensing*, 70(3):9. 10, 12, 75, 80

Höfle, B. and Pfeifer, N. (2007). Correction of laser scanning intensity data: Data and model-driven approaches. *ISPRS Journal of Photogrammetry and Remote Sensing*, 62(6):415 – 433. 6, 7, 75

Hopkinson, C., Chasmer, L. E., Sass, G., Creed, I. F., Sitar, M., Kalbfleisch, W., and Treitz, P. (2005). Vegetation class dependent errors in LiDAR ground elevation and canopy height estimates in a boreal wetland environment. *Canadian Journal of Remote Sensing*, 31(2):191–206. 75, 80

Hopkinson, C., Sitar, M., Chasmer, L., and Treitz, P. (2004). Mapping snowpack depth beneath forest canopies using airborne LiDAR. *Photogrammetric Engineering & Remote Sensing*, 70(3):323–330. 1, 12, 18, 21, 23, 24, 64, 65, 66, 67, 71, 74

J D Barnes Limited (2008). Greater toronto area: Orthoimagery 2008 [computer file]. 28, 40, 73

Kaasalainen, S., Ahokas, E., Hyyppä, J., and Suomalainen, J. (2005). Study of surface brightness from backscattered laser intensity: calibration of laser data. *Geoscience and Remote Sensing Letters, IEEE*, 2(3):255–259. 7

Kaasalainen, S., Kaartinen, H., and Kukko, A. (2008). Snow cover change detection with laser scanning range and brightness measurements. In *EARSeL eProceedings*, volume 7, pages 133–141. 22

Kaasalainen, S., Kaartinen, H., Kukko, A., Anttila, K., and Krooks, A. (2011). Application of mobile laser scanning in snow cover profiling. *Cryosphere*, 5(1):135–138. 21, 23

Kaasalainen, S., Kaasalainen, M., Mielonen, T., Suomalainen, J., Peltoniemi, J., and Naranen, J. (2006). Optical properties of snow in backscatter. *Journal of Glaciology*, 52(11):574–584. 18, 19

Kaasalainen, S., Karttunen, H., Piironen, J., Virtanen, J., Liljestrom, A., and Naranen, J. (2003). Backscattering from snow and ice: Laboratory and field measurements. *Canadian Journal of Physics*, 81(1-2):135–143. 19

Kim, H. H. (1992). Urban heat island. *International Journal of Remote Sensing*, 13(12):2319–2336. 16

Larsson, H., Steinvall, O., Chevalier, T., and Gustafsson, F. (2006). Characterizing laser radar snow reflection for the wavelengths 0.9 and 1.5 μm. *Optical Engineering*, 45(11):116201. 19

Liadsky, J. (2007). Introduction to LIDAR. In *NPS Lidar Workshop*, pages 1–41. 9

Maas, H. G. (2003). Planimetric and height accuracy of airborne laser scanner data: User requirements and system performance. In *Photogrammetric Week: Proceedings 49.*, pages 117–125. 10

Matheussen, B. V. and Thorolfsson, S. T. (2001). Urban Snow Surveys in Risvollan — Norway. In Brashear, R. W. and Maksimovic, C., editors, *Urban Drainage Modeling*, volume 275, pages 89–99. ASCE. 2, 18, 63, 81

McKay, G. A. and Gray, D. M. (1981). The distribution of snowcover. In Gray, D. M. and Male, D. H., editors, *Handbook of Snow: Principles, Processes, Management & Use*, chapter Part II: Snowfall and Snowcover, pages 3–13. Pergamon Press Canada, Toronto. 13, 14, 15, 27

Meng, X., Currit, N., and Zhao, K. (2010). Ground Filtering Algorithms for Airborne LiDAR Data: A Review of Critical Issues. *Remote Sensing*, 2:833–860. 36, 70

Meng, X., Wang, L., Silvn-Crdenas, J. L., and Currit, N. (2009). A multi-directional ground filtering algorithm for airborne LIDAR. *ISPRS Journal of Photogrammetry and Remote Sensing*, 64(1):117–124. 36

Moreno Baños, I., Garca, A. R., i Alavedra, J. M., i Figueras, P. O., na Iglesias, J. P., i Figueras, P. M., and López, J. T. (2011). Assessment of airborne LIDAR for snowpack depth modeling. *Bulletin of the Geological Society of Mexico*, 63:95–107. 1, 23, 24, 65, 66, 67

Mostafa, M. M. and Hutton, J. (2001). Direct positioning and orientation systems: How do they work? what is the attainable accuracy? In *Proceedings, American Society of Photogrammetry and Remote Sensing Annual Meeting*, pages 1–11. 9, 10, 11

Optech Inc. (2011a). ALTM Gemini: Summary Specification Sheet. Electronic. www.optech.ca Accessesed May 13th 2011. 7, 11, 19

Optech Inc. (2011b). LYNX M1: Summary Specification Sheet. Electronic. www.optech.ca Accessesed May 13th 2011. 23

Optech Inc. (2011c). Pegasus HD500: Summary Specification Sheet. Electronic. www.optech.ca Accessesed May 13th 2011. 6

Otake, K. (1980). Snow survey by aerial photographs. *GeoJournal*, 4(4):367–369. 18

Pomeroy, J. and Gray, D. (1995). Report no. 7 - snowcover: Accumulation, relocation and management. Technical report, National Hydrology Research Institute, Saskatoon, SK. 13, 14, 15

Prokop, A. (2008). Assessing the applicability of terrestrial laser scanning for spatial snow depth measurements. *Cold Regions Science and Technology*, 54(3):155 – 163. Snow avalanche formation and dynamics. 21, 22

Prokop, A., Schirmer, M., Rub, M., Lehning, M., and Stocker, M. (2008). A comparison of measurement methods: terrestrial laser scanning, tachymetry and snow probing for the determination of the spatial snow-depth distribution on slopes. *Annals of Glaciology*, 49(1):210–216. 22, 23

Rango, A. (1996). Spaceborne remote sensing for snow hydrology applications. *Hydrological Sciences*, 41:477–494. 2

Rees, W. G. (2006). *Remote Sensing of Snow and Ice.* CRC Press, Taylor and Francis Group. 13, 18

Ussyshkin, R. V., Boba, M., and Sitar, M. (2008). Performance Characterization of an aireborne LiDAR System: Bridging System Specifications and Expected Performance. In *The International Archives of the Photogrammetry, Remote Sensing and Spatial Information Sciences.*, volume 37, pages 177–182, Beijing. 68

Ussyshkin, R. V. and Smith, B. (2006). Performance Analysis of ALTM 3100EA: Instrument Specifications and Accuracy of LiDAR Data. In *ISPRS Conference Proceedings (Part B),*, pages 1–7, Paris, France. 10, 11, 69

Valeo, C. and Ho, C. L. I. (2004). Modelling urban snowmelt runoff. *Journal of Hydrology*, 299(3-4):237–251. 16

Viklander, M., Marsalek, J., Malmquist, P. A., and Watt, W. E. (2003). Urban drainage and highway runoff in cold climates: conference overview. *Water Science and Technology*, 48(9):1–10. 2, 64

Warren, S. G. (1982). Optical properties of snow. *Reviews Of Geophysics and Space Physics*, 20(1):67–89. 14, 19

Warren, S. G. and Wiscombe, W. J. (1980). A Model for the Spectral Albedo of Snow. II: Snow Containing Atmospheric Aerosols. *Journal of the Atmospheric Sciences*, 37(12):2734–2745. 20

Watson, F., Anderson, T., Kramer, M., Detka, J., Masek, T., Cornish, S., and Moore, S. (2008). Chapter 5 effects of wind, terrain, and vegetation on snow pack. In P.J., R. A. W. and Watson, F., editors, *The Ecology of Large Mammals in Central Yellowstone - Sixteen Years of Integrated Field Studies*, volume Volume 3, pages 67–84. Elsevier. 14, 15

Wehr, A. and Lohr, U. (1999). Airborne laser scanning-an introduction and overview. *ISPRS Journal of Photogrammetry and Remote Sensing*, 54(15):68–82. 1, 6, 7, 8, 9, 10

Zibordi, G., Meloni, G. P., and Frezzotti, M. (1996). Snow and ice reflectance spectra of the nansen ice sheet surfaces. *Cold Regions Science and Technology*, 24(2):147 – 151. 19

APPENDICES

Site 2010A

• Measured Depth

0 5 10   20
Meters

N

Site 2010B

• Measured Depth

0 12.5 25   50
Meters

N

Site 2010C

• Measured Depth

0   5   10   20
Meters

N

Site 2010D

• Measured Depth

0 5 10 20
Meters

Site 2010E

• Measured Depth

0 5 10 20
Meters

Site 2010F

• Measured Depth

0 5 10   20
Meters

N

Site 2011A

• Measured Depth

0   5   10   20
Meters

N

Site 2011B

•   Measured Depth

0   5   10   20

Meters

Site 2011C

•   Measured Depth

0   5 10   20

Meters

Site 2011D

• Measured Depth

N

0 5 10 20
Meters